공학박사 학위논문

Development of Multiple Reaction Monitoring-Mass Spectrometry based Proteome Multimarker Panel and Panel Development Software for the Detection of Hepatocellular Carcinoma

간암 진단을 위한 MRM-MS 기반의 단백체 다중 마커 패널 및 패널 개발 프로그램의 개발

2022년 8월

서울대학교 대학원
협동과정 바이오엔지니어링 전공

김 재 년

Ph. D. Dissertation

Development of Multiple Reaction Monitoring-Mass Spectrometry based Proteome Multimarker Panel and Panel Development Software for the Detection of Hepatocellular Carcinoma

August 2022

Interdisciplinary Program in Bioengineering
The Graduate School
Seoul National University

Jaenyeon Kim

Development of Multiple Reaction Monitoring-Mass Spectrometry based Proteome Multimarker Panel and Panel Development Software for the Detection of Hepatocellular Carcinoma

간암 진단을 위한 **MRM-MS** 기반의 단백체 다중 마커 패널 및 패널 개발 프로그램의 개발

지도 교수 김 영 수

이 논문을 공학박사 학위논문으로 제출함
2022년 06월

서울대학교 대학원
협동과정 바이오엔지니어링 전공
김 재 년

김재년의 공학박사 학위논문을 인준함
2022년 07월

위 원 장 최 진 욱 (인)
부위원장 김 영 수 (인)
위 원 신 현 무 (인)
위 원 한 도 현 (인)
위 원 박 준 호 (인)

Development of Multiple Reaction Monitoring-Mass Spectrometry based Proteome Multimarker Panel and Panel Development Software for the Detection of Hepatocellular Carcinoma

by
Jaenyeon Kim

Interdisciplinary Program in Bioengineering
The Graduate School
Seoul National University

This Dissertation is Approved for
The Degree of Doctor of Philosophy

July 2022

Approved by Thesis Committee:

Chair _____(Seal)
Jinwook Choi, MD., Ph. D.

Vice Chair _____(Seal)
Youngsoo Kim, Ph. D.

Examiner _____(Seal)
Hyun mu Shin, Ph. D.

Examiner _____(Seal)
Dohyun Han, Ph. D.

Examiner _____(Seal)
Joonho Park, Ph.D.

Abstract

Development of Multiple Reaction Monitoring-Mass Spectrometry based Proteome Multimarker Panel and Panel Development Software for the Detection of Hepatocellular Carcinoma

Jaenyeon Kim

Interdisciplinary Program in Bioengineering

The Graduate School

Seoul National University

Introduction: Conventional methods for the surveillance of hepatocellular carcinoma (HCC) by imaging, with and without serum tumor markers, are suboptimal with regard to accuracy. We aimed to develop and validate a reliable serum biomarker panel for the early detection of HCC using a proteomic technique. To simplify the computational process during the biomarker study aiming for clinical application, we developed two web application, one for marker panel development and the other for method validation.

Method: In Chapter 1, This multicenter case-control study comprised 727 patients with HCC (case group, n=393) and patients with risk factors (ie, cirrhosis, chronic hepatitis B, or chronic hepatitis C) but no HCC (control group, n=334). We developed a multiple reaction monitoring-mass spectrometry (MRM-MS) multimarker panel using 17 proteins from the sera of 398 patients (training set: 199 cases and 199 controls). Area under the receiver operating characteristics curve (AUROC) values of this MRM-MS panel with and without alpha-fetoprotein (AFP) and protein induced by vitamin K absence or antagonist-II (PIVKA-II) were compared in the training set and the independent test (n=170: 85 cases and 85 controls) and validation sets (n=159: 109 cases and 50 controls). In Chapter 2, web application for model development, Web Model Developer (WMD), were

programed with Python and Scikit Learn Module where web application was built with Django framework. Sample process methods regarding batch correction and transformation are provided. Forward, Backward and Recursive Feature Elimination options are available for feature selection with Logistic Regression or Support Vector Machine. Method Validation Portal (MVP), are designed with Spring boot, which was used as a framework for webpage development, which follows MVC Pattern. JSP, HTML, XML, and Java Script were used to develop the webpage. A server was composed of Apache Tomcat, MySQL. Input files were skyline-derived output files (csv file), and each files were organized by specific columns in order. SQL, JAVA were interworked to evaluate all the categories and show the results.

Results: In Chapter 1, The AUROC value of the MRM-MS panel that was combined with AFP and PIVKA-II was significantly higher than the standalone MRM-MS panel in the training (0.989 vs 0.937, $P<0.05$) and validation sets (0.958 vs 0.940, $P<0.05$) but not the test set (0.898 vs 0.891, $P=0.28$). The combination and standalone MRM-MS panels had higher AUROC values than AFP in the training (0.940 and 0.929 vs 0.775, both $P<0.05$), test (0.894 and 0.893 vs 0.593, both $P<0.05$), and validation sets (0.961 and 0.937 vs 0.806, both $P<0.05$) in detecting small (<2 cm) single HCC. The combination and standalone MRM-MS panels had significantly higher AUROC values than the GALAD score (0.945 and 0.931 vs 0.829, both $P<0.05$). In Chapter 2, WMD are provided as single webpage with Data process, Feature Selection and Model evaluation sections. WMD were able to process raw MRM data and suggest best set of features. The MVP portal reads a Skyline-output file and produces the following results: calibration curve, specificity, sensitivity, carryover, precision, recovery, matrix effect, dilution integrity, stability and QC according to the standards of each independent agency. The final tables and figures pertaining to the 11 evaluation categories are displayed in an individual page.

Conclusion: Our proteome 17-protein multimarker panel distinguished HCC patients from high-risk controls and had high accuracy in the early detection of HCC. Our web applications could have simplified the model development process and method evaluation process.

Keyword: hepatocellular carcinoma, biomarker, proteome, serum, software

Student Number: 2018-36314

List of Contents

List of Tables

Chapter 1

Chapter 2

List of Figures

Chapter 1

Chapter 2

List of abbreviations

HCC, hepatocellular carcinoma;

AFP, alpha-fetoprotein;

PIVKA-II, protein induced by vitamin K absence or antagonist-II;

LC, Liquid Chromatography;

MRM-MS, multiple reaction monitoring-mass spectrometry;

CHB, chronic hepatitis B;

CHC, chronic hepatitis C;

AUROC, area under the receiver operating characteristics curve;

LR, Logistic Regression;

SVM, Support Vector Machine;

RFE, Recursive Feature Elimination;

General Introduction

Hepatocellular carcinoma (HCC) accounts for 75% to 85% of all primary liver cancer cases, and its mortality rate is nearly equivalent to its global incidence(1). The burden of HCC is highest in East Asia, where cirrhosis, hepatitis B and C virus, and excessive alcohol consumption are the major risk factors(2).

Attempts to utilize protein biomarkers in clinical applications, including diagnosis, disease prognosis, therapeutic evaluations, and drug efficacy assessments were reported(3). Aspects of patient physiology, as tumor growth or disease conditions can be reflected by screening human plasma proteins. As one of less invasive diagnostic method, blood-based protein biomarkers is a promising source of disease indicator(4). Proteomic analysis by mass spectrometry (MS), in particular, multiple reaction monitoring method using liquid chromatography coupled mass spectrometry (MRM-LC/MS) has been widely applied to biomarker development for their high reproducibility, sensitivity and selectivity(5). Nonetheless, as MRM-LC/MS detects designated peptide of interest and fragmented ions, they are less affected with matrix effects With above mentioned characteristics of MRM-LC/MS, an MRM-LC/MS utilized assay may be suggested as a new clinical diagnostic tool to substitute conventional methods as antibody assays(6).

For MRM-MS based biomarker panel to become clinically ready, the study on performance of the multi marker panel and reproducibility of the sample preparation method have to be performed and well established. Computational manipulation is critical, which are both time-consuming and prone to error if processed with inefficient methods. After data collection, combination of feature

selected by machine learning algorithms needs to be discovered to represent the case/control, where importance of data processing prior to the process are immerging for a more statistically significant result. Where to appeal clinical reproducibility, analytical method evaluation is required specifically by administrations [US Food and Drug Administration (FDA), European Medicines Agency (EMA), and Korea Food and Drug Administration (KFDA)] for each marker presented in the multi marker panel. To date, there are no known application to guide through the marker panel development nor method validation required by the administrations. Solving fore mentioned computational procedures with more accessible environment, study on multi marker panel for clinical application could draw more attention to the fellow researchers and applied to many major diseases.

In chapter 1, the multicenter study aimed to develop and evaluate a new multimarker panel for the detection of HCC with target proteins using known biomarkers, examine whether the incorporation of AFP and PIVKA-II into the panel improves its accuracy, validate the panel in an independent cohort, and compare its performance with that of the GALAD score.

In the next chapter, two web applications to assist multi marker panel development and method evaluation are presented. The Web Model Developer (WMD), can process a 2-dimension sample-feature data with data normalization methods and suggests best feature combination to represent the data. The MRM-Method Validation Portal (M-MVP), which assists user to calculate and evaluate uploaded data corresponding to 11 categories of method valuation guideline published by FDA, EMA and KFDA.

Chapter 1.

Proteome Multimarker Panel for the Early Detection of Hepatocellular Carcinoma: Multicenter Derivation, Validation, and Comparison

1.1. Introduction

Although controversies exist over whether HCC surveillance programs provide a survival benefit for at-risk patients, a randomized controlled trial and several retrospective studies have concluded that surveillance through imaging studies, such as ultrasonography and serum alpha-fetoprotein (AFP) testing, results in early detection of HCC and reduced mortality(7-11). However, in a meta-analysis of patients with cirrhosis, abdominal ultrasonography, a universally recommended imaging modality for the surveillance of HCC, had a low sensitivity of 63% in detecting early-stage HCC with concomitant use of AFP(12). Considering the operator-dependent nature of ultrasonography and the high costs and potential physical harms of other imaging modalities (eg, radiation hazards with computed tomography), there is a need for the development of a highly sensitive yet economical and safe measure for the early detection of HCC(13).

The molecular heterogeneity of HCC has prompted attempts to integrate various serum biomarkers to detect the disease at an early stage(14). The GALAD score, which comprises age, sex, AFP, lectin-bound AFP, and protein induced by vitamin K absence or antagonist-II (PIVKA-II), is one of the most widely examined biomarker panels(15). Since the initial study, GALAD score were validated in various studies(16-20), granted with Breakthrough Device Designation by FDA(21).

Similarly, multiple reaction monitoring-mass spectrometry (MRM-MS), a targeted proteomic approach, quickly and accurately analyzes hundreds of proteins as potential biomarkers in various types of cancer(22-24). Our group has proposed

a multimarker panel for the detection of early-stage HCC, consisting of 28 proteins that have been identified by MRM-MS(25).

In this multi cohort study, we developed a multi marker panel with lesser proteins to distinguish HCC patients to high risk non-HCC controls. The developed cohort was validated by chronically independent data set and compared its performance to AFP and GALAD score.

1.2. Methods

1.2.1 Study design and participants

This case-control study was based on 2 independently established datasets of HCC patients and high-risk controls who selected per the same criteria from 3 referral centers [Seoul National University Hospital (SNUH), Asan Medical Center (AMC), and Samsung Medical Center (SMC)] in Seoul, Korea. The derivation set included 568 patients from all 3 participating centers—284 HCC patients and 284 non-HCC controls—whose serum samples were drawn between January 3, 2011 and September 3, 2013. They were randomly divided into the training set (199 HCC patients and controls each) and test set (85 HCC patients and controls each). The panel was developed and validated using these training and test sets, respectively. Serum samples were also drawn from 159 patients—109 HCC patients from SNUH and AMC and 50 non-HCC controls from AMC—between September 7, 2013 and August 3, 2020 to establish another independent validation set. (Figure 1-1)

Figure 1-1 Overview of development of the MRM-MS panel

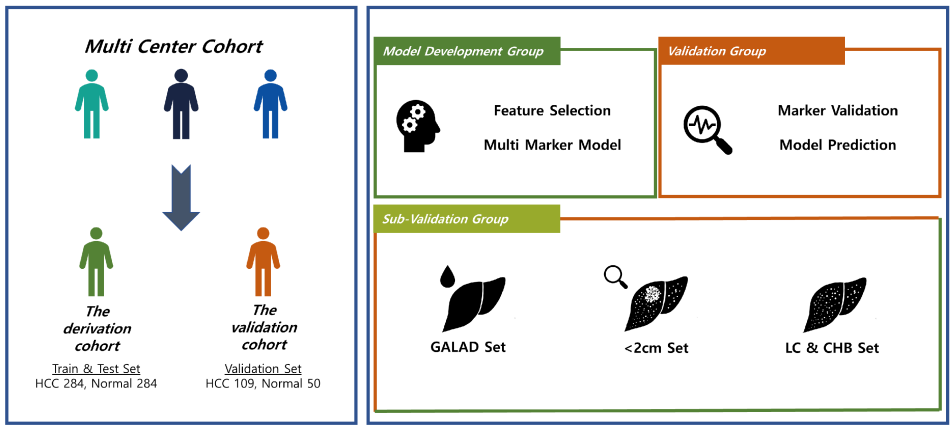

The study was performed with 2 independent cohorts: derivation and validation. A total of 383 target candidates were trained and internally validated with the derivation cohort, and the final 17-marker panel was validated with the validation cohort. Subgroups—tumor size under 2 cm, LC, and CHB—were also tested with regard to performance of the model.

Patients diagnosed with HCC were eligible if they were aged 20 to 80 years and diagnosed with single HCC that was smaller than 5 cm or 2–3 HCCs, each smaller than 3 cm, within 3 months prior to collection of their sera. The diagnosis of HCC was made according to radiographic or histological findings following the updated 2011 American Association for the Study of Liver Disease (AASLD) guidelines(26). Patients with radiological vascular invasion or extrahepatic metastasis of HCC by computed tomography (CT) or magnetic resonance (MRI) imaging, which detects advanced HCC, were excluded. The high-risk controls comprised patients aged 20 to 80 years with cirrhosis or chronic hepatitis B (CHB) or C (CHC) who were confirmed not to have had HCC by abdominal ultrasonography, computed tomography, or magnetic resonance imaging within 3 months prior to collection of their samples. Common exclusion criteria were (i) impaired hepatic function, defined as Child-Pugh class C; (ii) poor performance

status; considered an Eastern Cooperative Oncology Group performance status score of 3 or above; and (iii) any other malignancy within 3 years prior to the collection of sera.

Cirrhosis was diagnosed clinically per the following criteria: (i) histological findings, (ii) thrombocytopenia (<100,000/mm3) and a blunted, nodular liver edge with splenomegaly (>12 cm), or (iii) the presence of ascites, varices, or hepatic encephalopathy. CHB and CHC were defined as a positive serum hepatitis B surface antigen test and a positive serum anti-hepatitis C virus antibody test, respectively, on 2 separate occasions that were separated by at least 6 months.

This study was approved by the institutional review board of each participating center (Seoul National University Hospital, No. H-1710-028-891; Asan Medical Center, No. 2017-1049; Samsung Medical Center, No. 2017-08-164).

1.2.2 GALAD cohort

103 samples from independent validation cohort were analyzed for AFP and AFP-L3 level for GALAD score. The μTAS autoanalyzer (Wako Pure Chemical Industries) is an FDA clearance device for diagnosing HCC by measuring AFP and AFP-L3 concentrations. A sample load of 100 μL was analyzed for 9 min with a 2-min interval between each sample. The AFP-L3 concentration was calculated automatically as a percentage of total AFP and printed out. The quantifiable ranges of AFP and AFP-L3 were 0.3 to 4000.0 ng/mL and 0.5% to 99.5%, respectively, using a 2-point calibrator. All serum samples were measured following the manufacturer's instructions.

1.2.3 Biomarker Study

In a previous study, 383 peptides, corresponding to 176 proteins, had been identified as being suitable for quantitative MRM-MS analysis. Starting with 2189 proteins that were identified in 5 biobank resources, semiquantitative MRM-MS assay was performed on pooled serum samples of HCC patients and controls with cirrhosis or CHB, in which 23,184 peptides, representative of 1,693 proteins, were filtered by a proteomic approach using prediction servers and a database. Among 1583 reproducibly detectable peptides, 542 were differentially expressed in individual samples of HCC patients compared with controls, 421 of which were verified as being acceptable for subsequent screening according to pre-existing mass spectrometry spectral data. A subsequent quantitative MRM-MS analysis targeted 385 peptides that had undergone an interference screen using a stable isotope-labeled standard peptide mixture(27).

In this study, we performed MRM-MS quantification for 383 target peptides, correlating to 176 proteins, except for 2 peptides for which compatible stable isotope-labeled standard peptides were not obtained due to unavailability. Their exclusion did not affect the performance of the developed panel, because the 2 peptides were part of proteins that were represented by other peptides in the MRM-MS quantification. Screening methods of 383 targets are shown in Table 1-1.

1.2.4 Quantitative MRM-MS analysis

Prior to sample preparation, block randomization was performed to minimize the variance. A volume of 44 μL of each sample was mixed with 176 μL of MARS

buffer A (Agilent Technologies, CA) and passed through 0.22-μm Spin-X filters (Corning Costar, NY). The 6 most abundant proteins (albumin, immunoglobulin A, immunoglobulin G, transferrin, haptoglobin, and α1-antitrypsin) were removed from 200 μL of each sample mixture by a Multiple Affinity Removal System Human-6 (MARS Hu-6×100 mm; Agilent Technologies, Santa Clara, CA) column that was loaded onto a high-performance liquid chromatography system (Shimadzu Co., Kyoto, Japan). Five milliliters of each depleted sample was then concentrated on a 3000-Da molecular weight cutoff (MWCO) filter unit (Amicon Ultra-4 3K, Millipore, MA) in a precooled centrifuge at 4°C for 6 hours.

The protein in each depleted sample was quantified by bicinchoninic acid (BCA) assay, in which 2 mg/mL of BSA standard was diluted 1:2 6 times to generate a standard curve. Each sample was diluted 1:20 and 1:40 and loaded onto a 96-well plate. Further, 200 μL of a 1:50 mixture of copper solution and BCA solution was added and incubated at 37°C for 1 hour before scanning.

Samples were digested according to the results of the BCA assay. For a 100-μg digestion, each sample was adjusted with HPLC water to a volume of 20 μL. The adjusted sample was mixed with 20 μL of 0.2% RapiGest, 20 mM DTT, and 100 mM ABC buffer and reacted in 60°C for 1 hour. Next, 10 μL 100 mM iodoacetamide (IAA) was added and stored in the dark at room temperature for 30 minutes, after which 40 μL trypsin (Promega, sequencing-grade modified, Madison, WI) in 50 mM ABC was added to the mixture and incubated at 37°C for 4 hours. Finally, 10 μL 10% formic acid was added and incubated at 37°C to stop the reaction. Supernatants were collected after centrifugation at 15,000 rpm and 4°C.

Prior to the mass spectrometry analysis, each sample was spiked with stable isotope-labeled standard peptide (30% to 70% purity per the manufacturer, JPT,

Berlin, Germany) at a 9:1 ratio.

1.2.5 Capillary Liquid Chromatography

MRM-MS analysis was performed on a fully automated online 1260 Capillary-flow liquid chromatography (LC) system (Agilent Technologies, Santa Clara, CA, USA). The autosampler was set to 4 °C, where the LC separation was performed at 40 °C. Sample cleanup was performed using a guard column (2.1 × 15.0 mm, 1.8 μm, 80 Å), and peptides were separated on an analytical column (0.5 × 35.0 mm, 3.5 μm, 80 Å) (both columns from Agilent Technologies, Santa Clara, CA, USA).

Ten microliters of the digested sample were injected onto a guard column at 40 μL/min for a minute in 10% solvent B. Sample flow was directed from the guard to the analytical column after the valves were switched. Then, 10% solvent B was run at a flow rate of 40 μL/min for a minute. To separate the peptides, A linear gradient of 10% to 60% solvent B over 5 mins at 40 μL/min eluted bound peptides from the analytical column. The column wash was held at 90% solvent B for 1 min at 40 μL/min and then equilibrated at 10% solvent B for 4 mins. The switching valve was returned to its original position after a minute of equilibration, while reconditioning performed simultaneously in both guard and analytical columns.

1.2.6 Mass Spectrometry

Quantitative analysis was performed on an Agilent 6490 triple quadrupole (QqQ) mass spectrometer with an Electrospray source (Agilent Technologies,

Santa Clara, CA, USA), operated in positive ion, scheduled multiple reaction monitoring (MRM) mode. Gas temperature was set to 250 °C where gas flow as 15 L/min. Sheath gas temperature was set to 350 °C where the gas flows at 12 L/min. The delta electron multiplier voltage (EMV) was set to 200 V, and the cell accelerator voltage and fragment voltage were 5 V and 380 V, respectively.

1.2.7 Data preprocessing

Data transformation were performed for the normality of data distribution. Many statistical procedures assume that the variables are normally distributed. To ensure the normal distribution of each marker, data were transformed to log (x + 10–10). The skewness value for each marker in raw and log transform were calculated with the skewness function in the e1071 package of R. The absolute skewness value of the case group and the control group were calculated and added. The final data type for each marker were selected based on lower absolute skewness value, which the resulted in 233 raw data type and 150 log(x+10-10) data type. From proteins associated with multiple peptides, only a single peptide was selected on the basis of AUC and P values, to ensure that each peptide corresponded to a single protein (Figure 1-2)(28). We performed student's t test and calculated area under the receiver operating characteristics (AUROC) value for the transformed data of each peptide, leaving 107 peptides (79 proteins) with P <0.05 by student's t test and AUROC >0.6. Based on the P values and AUROC values, a single peptide was selected for each protein that was associated with multiple peptides. Consequently, 79 candidate proteins were included in the development of the panel.

Figure 1-2 Density plot of the 17 marker peptides in the MRM-MS panel

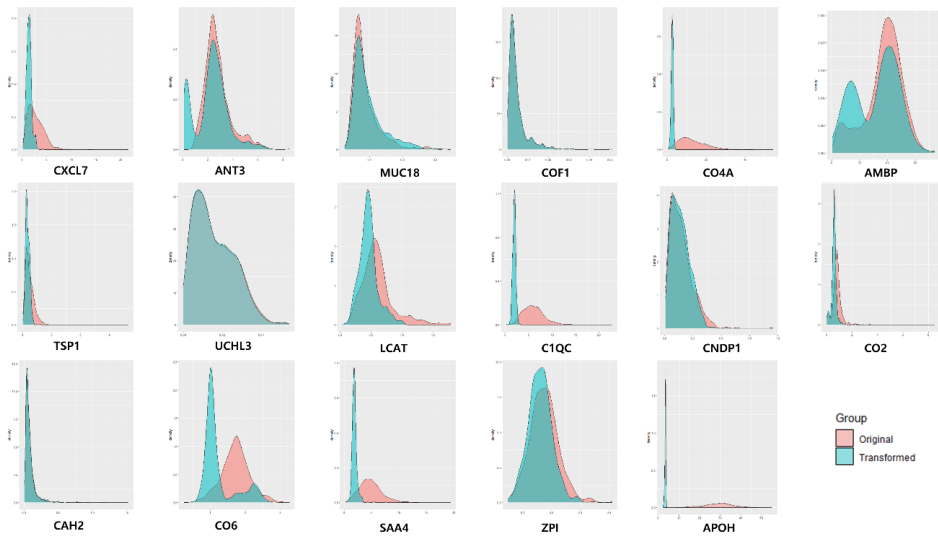

Density plot of raw and log ($x+10^{-10}$)-transformed data on the 17 markers. The less skewed format was used as the final transformation method.

1.2.8 Panel development and assessment

Protein expression levels were compared between HCC patients and controls in the training set for the 79 biomarker candidates by Mann-Whitney U test. We used logistic regression analysis to build the MRM-MS multimarker panel, with recursive feature elimination with crossvalidation to determine the markers that were to remain in the panel. AFP and PIVKA-II were later combined with the MRM-MS panel as continuous variables. The discriminatory abilities of AFP and the MRM-MS panel with and without AFP and/or PIVKA-II were evaluated by AUROC analysis. By DeLong test, we compared, in pairs, the AUROC values of the standalone MRM-MS panel, AFP, and the combination MRM-MS panels in the training, test, and validation sets, with that of the GALAD score in a subset (GALAD cohort) of the validation cohort(29). Youden index was used as the

optimal cutoff in training set and applied to test and validation set at which the sensitivity and specificity were calculated for the standalone MRM-MS and combination MRM-MS panels(30). The sensitivities and specificities were compared in each set with those of AFP at a cutoff of 20 ng/mL, a common value for screening HCC(31). All reported P values were two-sided, and P values less than 0.05 were deemed to be significant.

All statistical analyses were conducted in R (version 4.0.4; R development Core Team, Vienna, Austria; http://www.R-project.org) and SPSS (version 25.0; SPSS, Chicago, IL).

Table 1-1 MS Method Information of 383 targets

Protein	Precursor Mz	Precursor Charge	Product Mz	Product Charge	Fragment Ion
A1AG1_NWGLSVYADKPETTK	570.3	3	704.9	2	y13
A1AG1_SDVVYTDWK	556.8	2	811.4	1	y6
A1AT_	821.4	2	1103.6	1	y9
A1BG_LELHVDGPPPRPQLR	575.3	3	616.3	2	y11
A2AP_LGNQEPGGQTALK	656.8	2	771.4	1	y8
A2AP_LCQDLGPGAFR	617.3	2	604.3	1	y6
A2AP_QEDDLANINQWVK	524.9	3	674.4	1	y5
A2AP_DFLQSLK	425.7	2	588.4	1	y5
A2AP_LFGPDLK	395.2	2	529.3	1	y5
A2GL_DLLLPQPDLR	590.3	2	725.4	1	y6
A2GL_GQTLLAVAK	450.8	2	715.5	1	y7
A2MG_NEDSLVFVQTDK	697.8	2	836.5	1	y7
A2MG_TEHPFTVEEFVLPK	558.3	3	861.5	1	y7
A2MG_FEVQVTVPK	523.8	2	770.5	1	y7
A2MG_QGIPFFGQVR	574.8	2	850.5	1	y7
A2MG_TGTHGLLVK	309.2	3	412.8	2	y8
A2MG_AIGYLNTGYQR	628.3	2	1071.5	1	y9
A2MG_HYDGSYSTFGER	473.5	3	508.3	1	y4
A2MG_TEVSSNHVLIYLDK	540.0	3	694.4	2	y12
AFAM_YHYLIR	432.7	2	564.4	1	y4
ALBU_DLGEENFK	476.2	2	723.3	1	y6
ALBU_LVNEVTEFAK	575.3	2	937.5	1	y8
ALBU_SLHTLFGDK	339.9	3	465.8	2	y8
ALBU_LCTVATLR	467.3	2	660.4	1	y6
ALBU_DDNPNLPR	470.7	2	596.4	1	y5
ALBU_YLYEIAR	464.3	2	651.3	1	y5
ALBU_AAFTECCQAADK	686.3	2	1082.4	1	y9
ALBU_AACLLPK	386.7	2	630.4	1	y5
ALBU_LVTDLTK	395.2	2	577.3	1	y5
ALBU_QNCELFEQLGEYK	553.3	3	645.3	1	b5
ALBU_FQNALLVR	480.8	2	685.4	1	y6
ALBU_VPQVSTPTLVEVSR	504.6	3	589.3	1	y5
ALBU_RPCFSALEVDETYVPK	637.6	3	719.3	1	b6
ALBU_QTALVELVK	500.8	2	587.4	1	y5

Protein	Precursor Mz	Precursor Charge	Product Mz	Product Charge	Fragment Ion
ALS_ANVFVQLPR	522.3	2	759.5	1	y6
ALS_NLIAAVAPGAFLGLK	727.9	2	802.5	1	y8
ALS_LEYLLLSR	503.8	2	764.5	1	y6
ALS_LEALPNSLLAPLGR	732.4	2	1037.6	1	y10
AMBP_TVAACNLPIVR	607.3	2	1013.6	1	y9
AMBP_EYCGVPGDGDEELLR	854.9	2	1100.5	1	y10
ANGT_DPTFIPAPIQAK	649.4	2	724.4	1	y7
ANGT_VLSALQAVQGLLVAQGR	575.0	3	643.4	1	y6
ANGT_SLDFTELDVAAEK	719.4	2	975.5	1	y9
ANT3_VWELSK	381.2	2	662.4	1	y5
ANT3_VAEGTQVLELPFK	715.9	2	746.4	1	y6
ANT3_LPGIVAEGR	456.3	2	531.3	1	y5
APOA1_THLAPYSDELR	434.6	3	619.3	1	y5
APOA2_EPCVESLVSQYFQTVTDY GK	784.0	3	1062.5	2	y18
APOA2_SPELQAEAK	486.8	2	659.4	1	y6
APOA4_IDQNVEELK	544.3	2	974.5	1	y8
APOA4_ISASAEELR	488.3	2	775.4	1	y7
APOB_EVYGFNPEGK	570.3	2	911.4	1	y8
APOB_SVSLPSLDPASAK	636.3	2	885.5	1	y9
APOB_QGFFPDSVNK	569.8	2	659.3	1	y6
APOB_ALVDTLK	380.2	2	575.3	1	y5
APOB_SVGFHLPSR	333.9	3	407.2	2	y7
APOB_SGSSTASWIQNVDTK	790.9	2	1090.6	1	y9
APOB_LATALSLSNK	509.3	2	833.5	1	y8
APOB_AQIPILR	405.8	2	498.3	1	y4
APOB_TSSFALNLPTLPEVK	808.9	2	1010.6	1	y9
APOB_QIDDIDVR	487.3	2	732.4	1	y6
APOB_AASGTTGTYQEWK	700.3	2	911.4	1	y7
APOC2_TAAQNLYEK	519.3	2	865.4	1	y7
APOC2_TYLPAVDEK	518.3	2	658.3	1	y6
APOC3_DALSSVQESQVAQQAR	573.0	3	672.4	1	y6
APOC3_GWVTDGFSSLK	598.8	2	854.4	1	y8
APOC3_DYWSTVK	449.7	2	620.3	1	y5
APOC4_ELLETVVNR	536.8	2	717.4	1	y6
APOC4_AWFLESK	440.7	2	623.3	1	y5
APOD_IPTTFENGR	517.8	2	824.4	1	y7

Protein	Precursor Mz	Precursor Charge	Product Mz	Product Charge	Fragment Ion
APOE_AQAWGER	409.2	2	514.2	1	b5
APOF_SGVQQLIQYYQDQK	566.6	3	613.3	1	b6
APOH_ATVVYQGER	511.8	2	751.4	1	y6
APOL1_LNILNNNYK	553.3	2	765.4	1	y6
APOM_SLTSCLDSK	505.7	2	810.4	1	y7
APOM_AFLLTPR	409.3	2	599.4	1	y5
ATRN_CTWLIEGQPNR	687.3	2	813.4	1	y7
BAG6_EHIAASVSIPSEK	456.6	3	460.2	1	y4
BCDO2_VDIETLEK	473.8	2	732.4	1	y6
BGH3_DLLNNHILK	360.5	3	426.3	2	y7
BGH3_GDELADSALEIFK	704.4	2	993.5	1	y9
BTD_VDLITFDTPFAGR	726.4	2	1011.5	1	y9
BTD_ILSGDPYCEK	591.3	2	955.4	1	y8
BTD_LSSGLVTAALYGR	654.4	2	751.4	1	y7
C1QC_TNQVNSGGVLLR	629.3	2	815.5	1	y8
C1R_NIGEFCGK	462.7	2	697.3	1	y6
C1R_YTTEIIK	434.2	2	704.4	1	y6
C1R_ESEQGVYTCTAQGIWK	928.9	2	1227.6	1	y10
C1R_GYGFYTK	418.2	2	615.3	1	y5
C1RL_GSEAINAPGDNPAK	670.8	2	698.3	1	y7
C4BPA_DTIVFK	361.7	2	506.3	1	y4
C4BPA_TWYPEVPK	510.3	2	732.4	1	y6
C4BPB_ALLAFQESK	503.8	2	822.4	1	y7
CADH1_NTGVISVVTTGLDR	716.4	2	1060.6	1	y10
CAH1_GGPFSDSYR	493.2	2	627.3	1	y5
CAH1_YSSLAEAASK	513.8	2	776.4	1	y8
CAH1_VLDALQAIK	485.8	2	758.4	1	y7
CAH2_SADFTNFDPR	585.3	2	749.4	1	y6
CALR_FVLSSGK	369.2	2	491.3	1	y5
CATA_LFAYPDTHR	373.9	3	625.3	1	y5
CATA_DAQIFIQK	481.8	2	648.4	1	y5
CBPB2_YPLYVLK	448.3	2	732.5	1	y6
CBPB2_DTGTYGFLLPER	684.8	2	831.5	1	y7
CETP_ASYPDITGEK	540.8	2	759.4	1	y7
CFAB_DISEVVTPR	508.3	2	787.4	1	y7
CFAB_STGSWSTLK	483.7	2	778.4	1	y7

Protein	Precursor Mz	Precursor Charge	Product Mz	Product Charge	Fragment Ion
CFAB_VASYGVKPR	488.8	2	806.5	1	y7
CFAB_VSEADSSNADWVTK	754.8	2	1007.5	1	y9
CFAB_QLNEINYEDHK	468.2	3	485.2	1	b4
CFAH_EGWIHTVCINGR	481.2	3	619.3	1	y5
CFAI_FSVSLK	340.7	2	533.3	1	y5
CFAI_VFSLQWGEVK	596.8	2	946.5	1	y8
CHLE_NIAAFGGNPK	494.8	2	761.4	1	y8
CHLE_TQILVGVNK	486.3	2	742.5	1	y7
CHLE_IFFPGVSEFGK	614.3	2	967.5	1	y9
CHLE_AEEILSR	409.2	2	617.4	1	y5
CHLE_YLTLNTESTR	599.3	2	921.5	1	y8
CLUS_EIQNAVNGVK	536.3	2	829.5	1	y8
CLUS_TLLSNLEEAK	559.3	2	903.5	1	y8
CLUS_IDSLLENDR	537.8	2	846.4	1	y7
CLUS_ASSIIDELFQDR	697.4	2	922.4	1	y7
CLUS_RPHFFFPK	359.2	3	411.7	2	y6
CLUS_EILSVDCSTNNPSQAK	881.9	2	1221.5	1	y11
CLUS_ELDESLQVAER	644.8	2	802.4	1	y7
CLUS_ALQEYR	390.2	2	595.3	1	y4
CNDP1_ALEQDLPVNIK	620.4	2	798.5	1	y7
CNDP1_AIHLDLEEYR	420.2	3	467.2	1	y3
CO2_HAFILQDTK	358.2	3	469.3	1	b4
CO3_VVLVAVDK	421.8	2	644.4	1	y6
CO3_NEQVEIR	444.2	2	644.4	1	y5
CO4A_DSSTWLTAFVLK	684.4	2	791.5	1	y7
CO5_GGSASTWLTAFALR	719.4	2	1078.6	1	y9
CO6_SEYGAALAWEK	612.8	2	845.5	1	y8
CO6_ENPAVIDFELAPIVDLVR	670.7	3	811.5	1	y7
CO6_GFVVAGPSR	445.2	2	487.3	1	y5
CO6_QLEWGLER	515.8	2	789.4	1	y6
CO6_TLNICEVGTIR	425.9	3	446.3	1	y4
CO6A1_VAVVQYSGTGQQRPER	592.3	3	703.8	2	y12
CO6A2_LFAVAPNQNLK	607.8	2	713.4	1	y6
CO7_LSGNVLSYTFQVK	728.4	2	985.5	1	y8
CO7_ELSHLPSLYDYSAYR	605.3	3	774.3	1	y6
CO7_VLFYVDSEK	550.3	2	887.4	1	y7

Protein	Precursor Mz	Precursor Charge	Product Mz	Product Charge	Fragment Ion
CO7_QNDFNSVEEK	605.3	2	705.3	1	y6
CO7_AASGTQNNVLR	565.8	2	901.5	1	y8
CO8B_YEFILK	406.7	2	520.3	1	y4
CO8B_SGFSFGFK	438.7	2	585.3	1	y5
CO8B_IPGIFELGISSQSDR	540.3	3	679.3	1	y6
CO9_VVEESELAR	516.3	2	833.4	1	y7
CO9_TEHYEEQIEAFK	508.6	3	607.3	1	y5
CO9_TSNFNAAISLK	583.3	2	716.4	1	y7
CO9_DVVLTTTFVDDIK	733.4	2	938.5	1	y8
CO9_AIEDYINEFSVR	728.4	2	751.4	1	y6
COF1_NIILEEGK	458.3	2	688.4	1	y6
COL11_VFIGINDLEK	574.3	2	901.5	1	y8
CPN2_LSNNALSGLPQGVFGK	801.4	2	989.5	1	y10
CPN2_GQVVPALNEK	527.8	2	671.4	1	y6
CRP_ESDTSYVSLK	564.8	2	609.4	1	y5
CXCL7_NIQSLEVIGK	550.8	2	745.4	1	y7
CXCL7_GTHCNQVEVIATLK	523.9	3	773.5	1	y7
DOPO_TPEGLTLLFK	559.8	2	920.5	1	y8
DSG2_YKPTPIPIK	352.9	3	389.2	1	b3
ECM1_NLPATDPLQR	562.8	2	897.5	1	y8
ENPL_GVVDSDDLPLNVSR	743.4	2	1115.6	1	y10
ENTP5_ALLFEVK	410.3	2	635.4	1	y5
ESYT1_GSNPHLQTFTFTR	502.6	3	575.8	2	y9
EXT2_ASVVVPEEK	479.3	2	502.3	1	y4
FA7_TLAFVR	353.7	2	492.3	1	y4
FA9_NCELDVTCNIK	455.9	3	635.3	1	y5
FA9_SALVLQYLR	531.8	2	692.4	1	y5
FA9_VPLVDR	349.7	2	502.3	1	y4
FABPL_AIGLPEELIQK	605.9	2	856.5	1	y7
FAS_WVESLK	381.2	2	502.2	1	b4
FBLN1_GYHLNEEGTR	392.5	3	462.2	1	y4
FCG3A_AVVFLEPQWYR	704.4	2	749.4	1	y5
FCGBP_GNPAVSYVR	481.8	2	694.4	1	y6
FCGBP_LASVSVSR	409.7	2	634.4	1	y6
FCN3_GEPGDPVNLLR	583.8	2	711.5	1	y6
FCN3_SWSSYR	393.2	2	611.2	1	b5

Protein	Precursor Mz	Precursor Charge	Product Mz	Product Charge	Fragment Ion
FETA_GYQELLEK	490.3	2	759.4	1	y6
FETUA_QYGFCK	401.7	2	511.2	1	y4
FETUB_LVVLPFPK	456.8	2	700.4	1	y6
FHR1_TGESAEFVCK	564.3	2	840.4	1	y7
FHR2_ITCAEEGWSPTPK	738.3	2	772.4	1	y7
FHR2_TGDIVEFVCK	584.3	2	781.4	1	y6
FHR5_TGDAVEFQCK	577.8	2	711.3	1	y5
FIBA_VPPEWK	378.2	2	423.2	1	b4
FIBA_HPDEAAFFDTASTGK	531.9	3	621.3	1	b6
FIBA_GSESGIFTNTK	570.8	2	610.3	1	y5
FIBB_AHYGGFTVQNEANK	512.6	3	703.3	1	y6
FIBB_YQISVNK	426.2	2	560.3	1	y5
FIBG_DNCCILDER	597.7	2	965.4	1	y7
FINC_WSRPQAPITGYR	477.9	3	496.3	1	y4
FINC_LGVRPSQGGEAPR	441.9	3	605.8	2	y12
FINC_SYTITGLQPGTDYK	772.4	2	1079.5	1	y10
FINC_IYLYTLNDNAR	678.4	2	966.5	1	y8
FINC_FLATTPNSLLVSWQPPR	643.0	3	770.4	1	y6
FINC_IGDTWR	374.2	2	634.3	1	y5
FINC_HTSVQTTSSGSGPFTDVR	622.0	3	734.4	1	y6
FINC_IGDQWDK	431.2	2	748.3	1	y6
FINC_GEWTCIAYSQLR	495.2	3	503.3	1	y4
FUCO_DGLIVPIFQER	643.9	2	888.5	1	y7
G3BP1_INIPPQR	419.3	2	724.4	1	y6
G6PI_VFEGNRPTNSIVFTK	570.3	3	731.9	2	y13
GBLP_LWNTLGVCK	545.8	2	791.4	1	y7
GELS_TGAQELLR	444.3	2	658.4	1	y5
GPV_TLPAAAFR	423.7	2	632.4	1	y6
GPV_YLGVTLSPR	503.3	2	729.4	1	y7
GSHB_LFVDGQEIAVVYFR	552.6	3	584.3	1	y4
HABP2_GQCLITQSPPYYR	791.9	2	1011.5	1	y8
HBA_VGAHAGEYGAEALER	510.6	3	617.3	1	y5
HCDH_LVEVIK	350.7	2	488.3	1	y4
HEMO_GEFVWK	383.2	2	579.3	1	y4
HEMO_ELISER	373.7	2	391.2	1	y3
HEMO_QGHNSVFLIK	381.5	3	520.3	1	y4

Protein	Precursor Mz	Precursor Charge	Product Mz	Product Charge	Fragment Ion
HEP2_GPLDQLEK	450.2	2	632.3	1	y5
HEP2_GGETAQSADPQWEQLNNK	987.0	2	1156.6	1	y9
HEP2_LNILNAK	393.2	2	558.4	1	y5
HEP2_FAFNLYR	465.7	2	712.4	1	y5
HEP2_YEITTIHNLFR	469.6	3	557.8	2	y9
HEP2_NFGYTLR	435.7	2	609.3	1	y5
HEP2_SVNDLYIQK	540.3	2	893.5	1	y7
HEP2_QFPILLDFK	560.8	2	845.5	1	y7
HEP2_TLEAQLTPR	514.8	2	814.4	1	y7
HEP2_EVLLPK	349.7	2	357.2	1	y3
HEP2_IAIDLFK	410.3	2	706.4	1	y6
HEXA_TEIEDFPR	503.7	2	776.4	1	y6
HEXA_IQPDTIIQVWR	684.9	2	1127.6	1	y9
HGFA_LCNIEPDER	573.3	2	872.4	1	y7
HGFA_TTDVTQTFGIEK	670.3	2	923.5	1	y8
HGFA_VANYVDWINDR	682.8	2	818.4	1	y6
HPT_VGYVSGWGR	490.8	2	562.3	1	y5
HPT_VTSIQDWVQK	602.3	2	1003.5	1	y8
IBP3_ALAQCAPPPAVCAELVR	912.0	2	1208.6	1	y11
IBP3_FLNVLSPR	473.3	2	685.4	1	y6
IBP3_YGQPLPGYTTK	612.8	2	876.5	1	y8
ICAM1_VELAPLPSWQPVGK	760.9	2	1108.6	1	y10
IGF2_GIVEECCFR	585.3	2	900.3	1	y6
IGHM_YAATSQVLLPSK	639.4	2	1043.6	1	y10
IGHM_NVPLPVIAELPPK	693.9	2	1173.7	1	y11
IGHM_QIQVSWLR	515.3	2	561.3	1	y4
IGHM_QVGSGVTTDQVQAEAK	809.4	2	1090.5	1	y10
IGJ_IVLVDNK	400.7	2	588.3	1	y5
IGJ_SSEDPNEDIVER	695.3	2	971.5	1	y8
IGJ_IIVPLNNR	469.8	2	613.3	1	y5
IL1AP_LYIEYGIQR	577.8	2	878.5	1	y7
IL1AP_NEVWWTIDGK	624.3	2	905.5	1	y7
IPSP_AVVEVDESGTR	581.3	2	892.4	1	y8
ITB1_IGFGSFVEK	492.3	2	870.4	1	y8
ITIH1_QAVDTAVDGVFIR	695.9	2	805.5	1	y7
ITIH1_FAHYVVTSQVVNTANEAR	669.3	3	775.4	1	y7

Protein	Precursor Mz	Precursor Charge	Product Mz	Product Charge	Fragment Ion
ITIH1_EVAFDLEIPK	580.8	2	714.4	1	y6
ITIH1_AAISGENAGLVR	579.3	2	902.5	1	y9
ITIH1_LDAQASFLPK	545.3	2	861.5	1	y8
ITIH1_GSLVQASEANLQAAQDFVR	668.7	3	806.4	1	y7
ITIH2_VVNNSPQPQNVVFDVQIPK	708.0	3	945.5	1	y8
ITIH2_VQFELHYQEVK	473.9	3	596.8	2	y9
ITIH2_IYLQPGR	423.7	2	570.3	1	y5
ITIH2_AHVSFKPTVAQQR	490.3	3	630.9	2	y11
ITIH2_TILDDLR	423.2	2	631.3	1	y5
ITIH2_IQPSGGTNINEALLR	791.9	2	1157.6	1	y11
ITIH2_FYNQVSTPLLR	669.4	2	686.4	1	y6
ITIH3_EVSFDVELPK	581.8	2	934.5	1	y8
K2C1_SLVNLGGSK	437.8	2	674.4	1	y7
KAIN_VGSALFLSHNLK	429.2	3	593.8	2	y11
KAIN_LGFTDLFSK	514.3	2	914.5	1	y8
KAIN_WADLSGITK	495.8	2	733.4	1	y7
KAIN_FFSAQTNR	485.7	2	676.3	1	y6
KLKB1_DSVTGTLPK	459.3	2	616.4	1	y6
KLKB1_VLTPDAFVCR	589.3	2	864.4	1	y7
KNG1_TVGSDTFYSFK	626.3	2	1051.5	1	y9
KNG1_AATGECTATVGK	583.3	2	922.4	1	y9
KNG1_DFVQPPTK	466.2	2	669.4	1	y6
LCAT_SSGLVSNAPGVQIR	692.9	2	941.5	1	y9
LCAT_STELCGLWQGR	653.8	2	876.4	1	y7
LDHA_ISGFPK	324.7	2	535.3	1	y5
LG3BP_VEIFYR	413.7	2	598.3	1	y4
LG3BP_SLGWLK	352.2	2	503.3	1	y4
LG3BP_SDLAVPSELALLK	678.4	2	870.5	1	y8
LG3BP_AVDTWSWGER	603.8	2	634.3	1	y5
LG3BP_SQLVYQSR	490.8	2	765.4	1	y6
LMNB1_EYEAALNSK	512.8	2	532.3	1	y5
LUM_NNQIDHIDEK	409.2	3	435.2	2	y7
LUM_SLEDLQLTHNK	433.2	3	549.3	2	y9
LUM_SLEYLDLSFNQIAR	834.9	2	1063.6	1	y9
LUM_LPSGLPVSLLTLYLDNNK	653.0	3	766.4	1	y6
MBL2_FQASVATPR	488.8	2	701.4	1	y7

Protein	Precursor Mz	Precursor Charge	Product Mz	Product Charge	Fragment Ion
MMSA_AISFVGSNK	461.8	2	738.4	1	y7
MUC18_GATLALTQVTPQDER	533.9	3	644.3	1	y5
MUC18_EVTVPVFYPTEK	704.9	2	980.5	1	y8
MVP_LAQDPFPLYPGEVLEK	606.0	3	771.4	1	y7
NHRF1_LGVQVR	336.2	2	558.3	1	y5
P5CS_DEILLANK	458.3	2	471.2	1	b4
PEDF_GQWVTK	359.7	2	471.2	1	b4
PERM_VVLEGGIDPILR	640.9	2	840.5	1	y8
PHLD_VAFLTVTLHQGGATR	524.3	3	570.8	2	y11
PHLD_IADVTSGLIGGEDGR	730.4	2	1061.5	1	y11
PLGA_DVVLFEK	425.2	2	635.4	1	y5
PLMN_VYLSECK	449.7	2	636.3	1	y5
PLMN_WELCDIPR	544.8	2	773.4	1	y6
PLMN_HSIFTPETNPR	433.6	3	487.3	1	y4
PLMN_LFLEPTR	438.3	2	615.3	1	y5
PLMN_LSSPAVITDK	515.8	2	830.5	1	y8
PLMN_EAQLPVIENK	570.8	2	699.4	1	y6
PLMN_YEFLNGR	449.7	2	606.3	1	y5
PLTP_TGLELSR	388.2	2	504.3	1	y4
PON1_EVQPVELPNCNLVK	819.9	2	1282.7	1	y11
PON1_SFNPNSPGK	474.2	2	599.3	1	y6
PON1_STVELFK	412.2	2	635.4	1	y5
PON1_IFFYDSENPPASEVLR	628.6	3	868.5	1	y8
PON1_IQNILTEEPK	592.8	2	943.5	1	y8
PRDX2_ATAVVDGAFK	489.8	2	806.4	1	y8
PRDX2_TDEGIAYR	462.7	2	708.4	1	y6
PROC_ELNQAGQETLVTGWGYHSSR	745.0	3	874.9	2	y16
PROC_TFVLNFIK	491.3	2	733.5	1	y6
PROS_SFQTGLFTAAR	599.8	2	836.5	1	y8
PROS_FSAEFDFR	509.7	2	784.4	1	y6
PROS_NNLELSTPLK	564.8	2	787.5	1	y7
PROZ_ENFVLTTAK	511.8	2	533.3	1	y5
PSMD1_VSTAVLSITAK	545.3	2	731.5	1	y7
PVR_SVDIWLR	444.8	2	702.4	1	y5
QSOX1_SFYTAYLQR	574.8	2	751.4	1	y6
QSOX1_LAGAPSEDPQFPK	678.8	2	1044.5	1	y9

Protein	Precursor Mz	Precursor Charge	Product Mz	Product Charge	Fragment Ion
RET4_YWGVASFLQK	599.8	2	849.5	1	y8
RET4_LLNLDGTCADSYSFVFSR	689.0	3	742.4	1	y6
RET4_DPNGLPPEAQK	583.3	2	669.4	1	y6
S10AD_SLDVNQDSELK	624.3	2	833.4	1	y7
SAA4_GPGGVWAAK	421.7	2	688.4	1	y7
SAA4_FRPDGLPK	310.5	3	573.3	1	b5
SAE2_ESVLQFYPK	555.8	2	795.4	1	y6
SAMP_IVLGQEQDSYGGK	697.4	2	1068.5	1	y10
SEPP1_QPPAWSIR	477.8	2	729.4	1	y6
SEPP1_DDFLIYDR	528.8	2	566.3	1	y4
SEPP1_VSLATVDK	416.7	2	733.4	1	y7
SHBG_TSSSFEVR	456.7	2	637.3	1	y5
SHBG_TWDPEGVIFYGDTNPK	613.6	3	941.4	1	y8
SHBG_QVSGPLTSK	458.8	2	689.4	1	y7
SHBG_IALGGLLFPASNLR	721.4	2	804.4	1	y7
SHBG_QAEISASAPTSLR	665.9	2	889.5	1	y9
SHBG_DIPQPHAEPWAFSLDLGLK	712.0	3	953.5	2	y17
SODE_AGLAASLAGPHSIVGR	492.9	3	618.3	2	y13
SPRC_YIPPCLDSELTEFPLR	650.7	3	837.4	2	y14
SSRP1_ELQCLTPR	508.8	2	646.3	1	y5
SYEP_LLSVNIR	407.8	2	588.3	1	y5
TFR1_VEYHFLSPYVSPK	522.6	3	690.4	1	y6
THBG_NALALFVLPK	543.3	2	787.5	1	y7
THBG_GWVDLFVPK	530.8	2	817.5	1	y7
THRB_SEGSSVNLSPPLEQCVPDR	1036.0	2	1210.6	1	y10
THRB_ELLESYIDGR	597.8	2	710.3	1	y6
THRB_SPQELLCGASLISDR	823.4	2	978.5	1	y9
THRB_ETWTANVGK	503.3	2	589.3	1	y6
TRFE_DGAGDVAFVK	489.7	2	735.4	1	y7
TRFE_EFQLFSSPHGK	426.2	3	612.3	1	y6
TRFE_SASDLTWDNLK	625.3	2	776.4	1	y6
TRFE_EGYYGYTGAFR	642.3	2	771.4	1	y7
TRFE_NPDPWAK	414.2	2	501.3	1	y4
TRFE_YLGEEYVK	500.8	2	724.4	1	y6
TSP1_SITLFVQEDR	604.3	2	793.4	1	y6
TSP1_DLASIAR	373.2	2	517.3	1	y5

Protein	Precursor Mz	Precursor Charge	Product Mz	Product Charge	Fragment Ion
TSP1_TIVTTLQDSIR	623.9	2	933.5	1	y8
TSP1_GTSQNDPNWVVR	686.8	2	770.4	1	y6
TTC37_DFNCWESLGEAYLSR	616.3	3	738.4	1	y6
TTHY_VLDAVR	336.7	2	460.3	1	y4
TTHY_AADDTWEPFASGK	697.8	2	921.4	1	y8
UCHL3_YLENYDAIR	578.8	2	880.4	1	y7
VCAM1_NTVISVNPSTK	580.3	2	845.5	1	y8
VCAM1_LTAFPSESVK	539.8	2	646.3	1	y6
VIGLN_INIPPPSVNR	553.8	2	766.4	1	y7
VIME_SSVPGVR	351.2	2	527.3	1	y5
VTDB_FPSGTFEQVSQLVK	522.9	3	574.4	1	y5
VTDB_VCSQYAAYGEK	638.3	2	1016.5	1	y9
VTDB_LCDNLSTK	475.7	2	837.4	1	y7
VTDB_VLEPTLK	400.2	2	458.3	1	y4
VTNC_CTEGFNVDK	535.2	2	909.4	1	y8
VTNC_GQYCYELDEK	652.8	2	956.4	1	y7
VTNC_DVWGIEGPIDAAFTR	823.9	2	1076.5	1	y10
VTNC_GSQYWR	398.7	2	524.3	1	y3
VTNC_FEDGVLDPDYPR	711.8	2	875.4	1	y7
VTNC_QPQFISR	438.2	2	522.3	1	y4
VTNC_VDTVDPPYPR	579.8	2	629.3	1	y5
VWF_AVSPLPYLR	508.3	2	548.3	1	y4
VWF_VTVFPIGIGDR	587.3	2	727.4	1	y7
ZA2G_SSGAFWK	391.7	2	608.3	1	y5
ZPI_LFDEINPETK	603.3	2	945.5	1	y8

1.3. Results

1.3.1 Characteristics of the study population

Most participants had cirrhosis (62.3%, 65.9%, and 82.6% for HCC patients and 78.9%, 75.3%, and 100.0% for controls in the training, test, and validation sets, respectively) and Child-Pugh class A liver function (92.4%, 89.4%, and 96.3% and 87.9%, 89.4%, and 70.0%, respectively). All HCC patients with noncirrhotic liver, except 1 in the validation set, had CHB or CHC. No participant had a coinfection with hepatitis B and C viruses. Most HCC patients had a single tumor (90.5%, 89.4%, and 82.6% in the training, test, and validation sets, respectively) (Table 1-2).

Table 1-2 Characteristics of the study population

	Training set			Test set			Validation set		
	HCC (n=199)	Control (n=199)	P value	HCC (n=85)	Control (n=85)	P value	HCC (n=109)	Control (n=50)	P value
Age, years	58.0 (52.0–64.0)	56.0 (51.5–61.0)	0.010	58.0 (50.0–63.0)	56.0 (52.0–64.0)	0.332	61.0 (56.0–67.0)	57.0 (51.0–61.0)	0.001
Sex, N (%)			<0.001			0.007			<0.001
Female	34 (17.1%)	80 (40.2%)		23 (27.1%)	41 (48.2%)		17 (15.6%)	26 (52.0%)	
Male	165 (82.9%)	119 (59.8%)		62 (72.9%)	44 (51.8%)		92 (84.4%)	24 (48.0%)	
Body mass index, kg/m²	24.7 (22.5–26.7)	24.4 (22.3–26.5)	0.504	24.8 (22.6–26.3)	24.0 (22.4–25.8)	0.161	24.5 (22.5–26.6)	24.4 (23.0–27.9)	0.765
Platelet, ×10³/μL	142.0 (112.5–175.0)	87.0 (65.0–127.0)	<0.001	140.0 (110.0–180.0)	92.0 (64.0–147.0)	<0.001	140.0 (102.0–186.0)	74.0 (56.0–102.0)	<0.001
Creatinine, mg/dL	0.9 (0.8–1.0)	0.8 (0.6–0.9)	<0.001	0.8 (0.8–1.0)	0.8 (0.6–0.9)	0.002	0.9 (0.7–1.0)	0.7 (0.6–0.9)	<0.001
Albumin, g/dL	3.8 (3.5–4.0)	4.2 (3.8–4.5)	<0.001	3.8 (3.4–4.0)	4.4 (4.0–4.6)	<0.001	3.8 (3.6–4.1)	3.9 (3.7–4.3)	0.829
ALT, IU/L	41.0 (26.0–114.5)	23.0 (17.0–33.0)	<0.001	51.0 (28.0–121.0)	26.0 (18.0–35.0)	<0.001	26.0 (19.0–36.0)	23.0 (19.0–30.0)	0.236
Total bilirubin, mg/dL	0.9 (0.5–1.2)	1.1 (0.7–1.6)	<0.001	0.9 (0.6–1.3)	1.0 (0.8–1.4)	0.115	0.7 (0.5–0.9)	1.6 (1.0–2.3)	<0.001
Prothrombin time, INR	1.1 (1.0–1.2)	1.1 (1.0–1.2)	<0.001	1.2 (1.1–1.3)	1.1 (1.0–1.2)	<0.001	1.1 (1.0–1.1)	1.1 (1.1–1.3)	<0.001
Risk factors			<0.001			0.346			0.004
Cirrhosis, N (%)	124 (62.3%)	157 (78.9%)		56 (65.9%)	64 (75.3%)		90 (82.6%)	50 (100.0%)	
Noncirrhotic CHB, N (%)	65 (32.7%)	34 (17.1%)		20 (23.5%)	16 (18.8%)		15 (13.8%)	0	

	Training set			Test set			Validation set		
	HCC (n=199)	Control (n=199)	P value	HCC (n=85)	Control (n=85)	P value	HCC (n=109)	Control (n=50)	P value
Noncirrhotic CHC, N (%)	10 (5.0%)	8 (4.0%)		9 (10.6%)	5 (5.9%)		3 (2.8%)	0	
Others, N (%)	0			0			1 (0.9%)		
Child-Pugh class, N (%)			0.183			1.000			<0.001
A	183 (92.4%)	175 (87.9%)		76 (89.4%)	76 (89.4%)		105 (96.3%)	35 (70.0%)	
B	15 (7.6%)	24 (12.1%)		9 (10.6%)	9 (10.6%)		4 (3.7%)	15 (30.0%)	
Alcoholic, N (%)	20 (10.1%)	12 (6.0%)	0.197	6 (7.1%)	8 (9.4%)	0.780	14 (12.8%)	6 (12.0%)	1.000
Diabetes mellitus, N (%)	45 (22.6%)	19 (9.5%)	0.001	11 (12.9%)	5 (5.9%)	0.189	30 (27.5%)	5 (10.0%)	0.023
Hypertension, N (%)	60 (30.2%)	13 (6.5%)	<0.001	17 (20.0%)	7 (8.2%)	0.047	34 (31.2%)	13 (26.0%)	0.632
AFP ng/mL, median (IQR)	6.0 (2.9–14.1)	2.5 (1.7–3.8)	<0.001	5.7 (2.7–19.3)	2.8 (2.0–3.9)	<0.001	10.9 (3.5–43.9)	3.0 (2.3–5.6)	<0.001
PIVKA-II mAU/mL, median (IQR)	32.0 (23.0–83.5)	16.0 (13.0–20.0)	<0.001	37.0 (23.0–78.0)	16.0 (13.0–20.0)	<0.001	42.0 (26.0–216.0)	17.0 (14.0–21.0)	<0.001
Tumor number, N (%)									
1	180 (90.5%)			76 (89.4%)			90 (82.6%)		
2	12 (6.0%)			6 (7.1%)			15 (13.8%)		
3	7 (3.5%)			3 (3.5%)			4 (3.7%)		
Tumor size, cm	2.4 (1.6–3.0)			2.4 (1.5–3.7)			2.5 (1.5–3.2)		
AJCC stage, n (%)									

	Training set			Test set			Validation set		
	HCC (n=199)	Control (n=199)	P value	HCC (n=85)	Control (n=85)	P value	HCC (n=109)	Control (n=50)	P value
IA	77 (38.7%)			31 (36.5%)			42 (38.5%)		
IB	105 (52.8%)			45 (52.9%)			48 (44.0%)		
II	17 (8.5%)			9 (10.6%)			19 (17.4%)		

Data are provided in N (%) or median (interquartile range). HCC, hepatocellular carcinoma; ALT, alanine aminotransferase; INR, international normalized ratio; CHB, chronic hepatitis B; CHC, chronic hepatitis C; AFP, alpha-fetoprotein; PIVKA-II, protein induced by vitamin K absence or antagonist-II; AJCC, American Joint Committee on Cancer; IQR, interquartile range.

1.3.2 Development of an MRM-MS panel

Of the 79 candidate proteins that were significantly associated with the presence of HCC ($P<0.05$), 17 proteins [PPBP (platelet basic protein), SERPINC1 (antithrombin-III), MCAM (cell surface glycoprotein), CFL1 (cofilin-1), C4A (complement C4-A), AMBP (protein AMBP), THBS1 (thrombospondin-1), UCHL3 (ubiquitin carboxyl-terminal hydrolase isozyme L3), LCAT (phosphatidylcholine-sterol acyltransferase), C1QC (complement C1q subcomponent subunit C), CNDP1 (Beta-Ala-His dipeptidase), C2 (cytochrome c oxidase subunit 2), CA2 (carbonic anhydrase 2), C6 (complement component C6), SAA4 (serum amyloid A-4 protein), SERPINA10 (protein Z-dependent protease inhibitor), and APOH (beta-2-glycoprotein 1)] were selected as optimal constituents of the MRM-MS panel by stepwise selection. The predicted probability of HCC cases according to the panel was calculated in the training set (Table 1-3).

Table 1-3 Logistic regression equation (logit [P=HCC]) with selective log transformation for the 17 marker proteins

Protein (gene name)	Peptide sequence	Transformation	Coefficient
(Intercept)			-1.977
PPBP	NIQSLEVIGK	Log ($x+10^{-10}$)	1.714
SERPINC1	VWELSK	Normal	-1.48
MCAM	EVTVPVFYPTEK	Log ($x+10^{-10}$)	-22.293
CFL1	NIILEEGK	Normal	141.879
C4A	DSSTWLTAFVLK	Log ($x+10^{-10}$)	1.175
AMBP	TVAACNLPIVR	Log ($x+10^{-10}$)	0.034
THBS1	GTSQNDPNWVVR	Log ($x+10^{-10}$)	2.614
UCHL3	YLENYDAIR	Normal	32.042
LCAT	SSGLVSNAPGVQIR	Log ($x+10^{-10}$)	-10.386
C1QC	TNQVNSGGVLLR	Log ($x+10^{-10}$)	-2.258
CNDP1	AIHLDLEEYR	Log ($x+10^{-10}$)	2.839
C2	HAFILQDTK	Log ($x+10^{-10}$)	5.261
CA2	SADFTNFDPR	Log ($x+10^{-10}$)	22.593
C6	QLEWGLER	Log ($x+10^{-10}$)	1.005
SAA4	GPGGVWAAK	Log ($x+10^{-10}$)	-2.048
SERPINA10	LFDEINPETK	Log ($x+10^{-10}$)	19.721
APOH	ATVVYQGER	Normal	0.078

PPBP, platelet basic protein; SERPINC1, antithrombin-III; MCAM, cell surface glycoprotein; CFL1, cofilin-1; C4A, complement C4-A; AMBP, protein AMBP; THBS1, thrombospondin-1; UCHL3, ubiquitin carboxyl-terminal hydrolase isozyme L3; LCAT, phosphatidylcholine-sterol acyltransferase; C1QC, complement C1q subcomponent subunit C; CNDP1, Beta-Ala-His dipeptidase; C2, cytochrome c oxidase subunit 2; CA2, carbonic anhydrase 2; C6, complement component C6; SAA4, serum amyloid A-4 protein; SERPINA10, protein Z-dependent protease inhibitor; APOH, beta-2-glycoprotein 1.

1.3.3 Performance of the MRM-MS panel with and without AFP and PIVKA-II in detecting HCC

In the training set, the standalone MRM-MS panel had a significantly higher AUROC value (0.937 vs 0.759; P <0.001) than AFP alone. At the optimal cutoff of 20 ng/mL per the Youden index, the MRM-MS panel had greater sensitivity (80.4% vs 17.1%) and lower specificity (93.5% vs 97.5%) than AFP. The addition of AFP to the MRM-MS panel (designated as the MA panel) improved the AUROC value (0.949; 95% CI, 0.929–0.969; P=0.006), whereas that of PIVKA-II to it (the MP panel) did not (0.941; 95% CI, 0.920–0.963; P=0.073). The combination MRM-MS panel with AFP and PIVKA-II (the MAP panel) had a significantly higher AUROC value (0.953; 95% CI, 0.934–0.971; P=0.002), similar sensitivity (80.4%), and greater specificity (96.5%) compared with the standalone MRM-MS panel. (Figure 1-3)

Figure 1-3 Performance of AFP and the MRM-MS panel with and without AFP and PIVKA-II in detecting HCC.

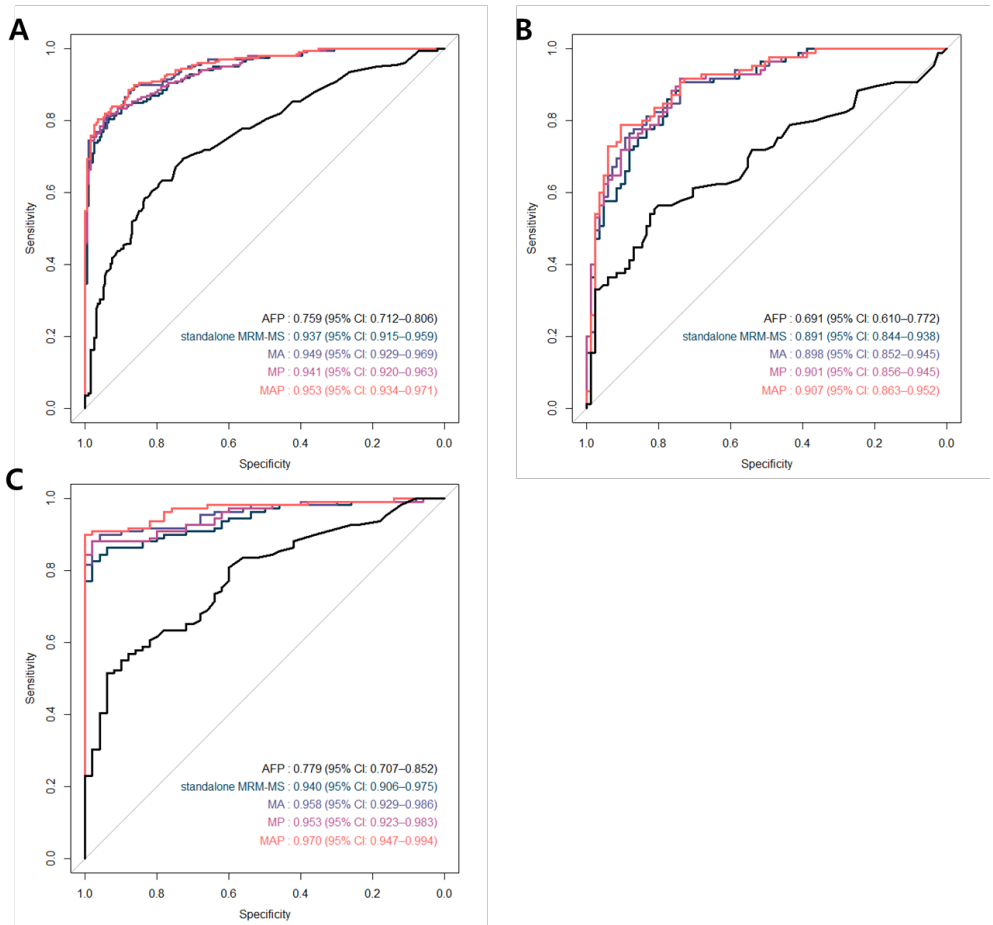

ROC curves of AFP, standalone MRM-MS panel, MRM-MS + AFP (MA) panel, MRM-MS + PIVKA-II (MP) panel, and MRM-MS + AFP + PIVKA-II (MAP) panel in the (A) training set, (B) test set, and (C) validation set.

In the test set, the MRM-MS panel yielded a significantly higher AUROC value (0.891 vs 0.691; P<0.001), greater sensitivity (78.8% vs 24.7%), and lower specificity (81.2% vs 97.7%) than AFP. The AUROC values of the MA (0.891; 95% CI, 0.844–0.938; P=0.598), MP (0.901; 95% CI, 0.856–0.945; P=0.086), and MAP panels (0.907; 95% CI, 0.863–0.952; P=0.280) were comparable with that of the standalone MRM-MS panel. However, the sensitivity and specificity were higher in the MAP panel (81.2% and 82.3%, respectively) versus the standalone MRM-MS panel.

In the validation set, the MRM-MS panel had a significantly higher AUROC value (0.940 vs 0.779, P <0.001), higher sensitivity (88.1% vs 35.8%), and lower specificity (82.0% vs 96.0%) than AFP. The AUROC values of the MA (0.958; 95% CI, 0.929–0.986; P=0.004), MP (0.953; 95% CI, 0.923–0.983; P=0.001), and MAP panels (0.970; 95% CI, 0.947–0.994; P <0.001) were also higher than that of the standalone MRM-MS panel. The sensitivity and specificity of the MAP panel were 89.9% and 98.0%, respectively—both higher compared with the standalone MRM-MS panel (Table 1-4).

Table 1-4 Performance of AFP and the MRM-MS panel with and without AFP and PIVKA-II in detecting HCC

	AUROC 95% CI	P value	Sensitivity (%)	Specificity (%)
Training set				
AFP	0.759 (0.712–0.806)		17.1	97.5
Standalone MRM-MS panel	0.937 (0.915–0.959)	<0.001*	80.4	93.5
MA panel	0.949 (0.929–0.969)	0.006†	88.4	87.5
MP panel	0.941 (0.920–0.963)	0.073†	81.4	94.5
MAP panel	0.953 (0.934–0.971)	0.002†	80.4	96.5
Test set				
AFP	0.691 (0.610–0.772)		24.7	97.7
Standalone MRM-MS panel	0.891 (0.844–0.938)	<0.001*	78.8	81.2
MA panel	0.898 (0.852–0.945)	0.598†	89.4	74.1
MP panel	0.901 (0.856–0.945)	0.086†	81.2	78.8
MAP panel	0.907 (0.863–0.952)	0.280†	81.2	82.3
Validation set				
AFP	0.779 (0.707–0.852)		35.8	96.0
Standalone MRM-MS panel	0.940 (0.906–0.975)	<0.001*	88.1	82.0
MA panel	0.958 (0.929–0.986)	0.004†	92.7	70.0
MP panel	0.953 (0.923–0.983)	0.001†	88.1	98.0
MAP panel	0.970 (0.947–0.994)	<0.001†	89.9	98.0

* AUROC of the standalone MRM-MS panel versus AUROC of AFP. † AUROC of MA, MP, or MAP panel versus AUROC of the standalone MRM-MS panel. AUROC- area under the receiver operating characteristics curve; AFP- alpha-fetoprotein; MA- multiple reaction monitoring-mass spectrometer + AFP; MP- multiple reaction monitoring-mass spectrometer + protein induced by vitamin K absence or antagonist-II; MAP- multiple reaction monitoring-mass spectrometer + AFP + protein induced by vitamin K absence or antagonist-II.

1.3.4 Performance of the MRM-MS panel with and without AFP and PIVKA-II vs GALAD in detecting HCC

The GALAD score was introduced as a substitute for conventional AFP method and were granted with Breakthrough Device Designation by FDA(21). For the multi marker panel to be suggested to clinical stage, performance comparison between GALAD score and the panel were inevitable.

The GALAD cohort was a subset of the validation set and was composed of 53 HCC patients and 50 controls from a single participating center (AMC) (Table 1-6). The MRM-MS panel had a significantly higher AUROC value (0.931 vs 0.718; P <0.001), greater sensitivity (88.7% vs 52.8%), and lower specificity (82.0% vs 92.0%) than the GALAD score. The AUROC value of the MAP panel was significantly higher (0.958; 95% CI, 0.916–1.000; P=0.009) than the standalone MRM-MS panel (Figure 1-5). The addition of AFP and PIVKA-II to the MRM-MS panel improved its sensitivity (90.6%) and specificity (98.0%) (Table 1-7). Combining AFP, and PIVKA-II, the marker panel could have outperformed GALAD score in both sensitivity and specificity.

Table 1-5 Characteristics of the GALAD cohort

	HCC (n=53)	Control (n=50)	P value
Age, years	60.0 (52.0–66.0)	57.0 (51.0–61.0)	0.072
Sex, N (%)			<0.001
Female	7 (13.2%)	26 (52.0%)	
Male	46 (86.8%)	24 (48.0%)	
Body mass index, kg/m^2	25.2 (22.5–27.1)	24.4 (23.0–27.9)	0.791
Platelet, x10^3/μL	162.0 (121.0–192.0)	74.0 (56.0–102.0)	<0.001
Creatinine, mg/dL	0.9 (0.8–1.0)	0.7 (0.6–0.9)	<0.001
Albumin, g/dL	3.8 (3.6–4.1)	3.9 (3.7–4.3)	0.437
ALT, IU/L	22.0 (18.0–37.0)	23.0 (19.0–30.0)	0.685
Total bilirubin, mg/dL	0.6 (0.4–0.8)	1.6 (1.0–2.3)	<0.001
Prothrombin time, INR	1.1 (1.0–1.1)	1.1 (1.1–1.3)	<0.001
Risk factors			0.001
Cirrhosis, N (%)	42 (79.2%)	50 (100.0%)	
Noncirrhotic CHB, N (%)	9 (17.0%)	0	
Noncirrhotic CHC, N (%)	2 (3.8%)	0	
Others, N (%)	0		
Child-Pugh class, N (%)			0.003
A	50 (94.3%)	35 (70.0%)	
B	3 (5.7%)	15 (30.0%)	
Alcoholic, N (%)	4 (7.5%)	6 (12.0%)	0.518
Diabetes mellitus, N (%)	14 (26.4%)	5 (10.0%)	0.058
Hypertension, N (%)	18 (34.0%)	13 (26.0%)	0.506
AFP, ng/mL	6.8 (3.0–58.1)	3.0 (2.3–5.6)	<0.001
PIVKA-II, mAU/mL	68.0 (27.0–241.0)	17.0 (14.0–21.0)	<0.001
Tumor number, N (%)			

	HCC (n=53)	Control (n=50)	P value
1	47 (88.7%)		
2	4 (7.5%)		
3	2 (3.8%)		
Tumor size, cm	2.5 (1.9–3.5)		
AJCC stage, n (%)			
IA	17 (32.1%)		
IB	30 (56.6%)		
II	6 (11.3%)		

Data are provided as N (%) or median (interquartile range). HCC, hepatocellular carcinoma; ALT, alanine aminotransferase; INR, international normalized ratio; CHB, chronic hepatitis B; CHC, chronic hepatitis C; AFP, alpha-fetoprotein; PIVKA-II, protein induced by vitamin K absence or antagonist-II; AJCC, American Joint Committee on Cancer.

Figure 1-4 Performance of GALAD score and the MRM-MS panel with and without AFP and PIVKA-II in detecting HCC

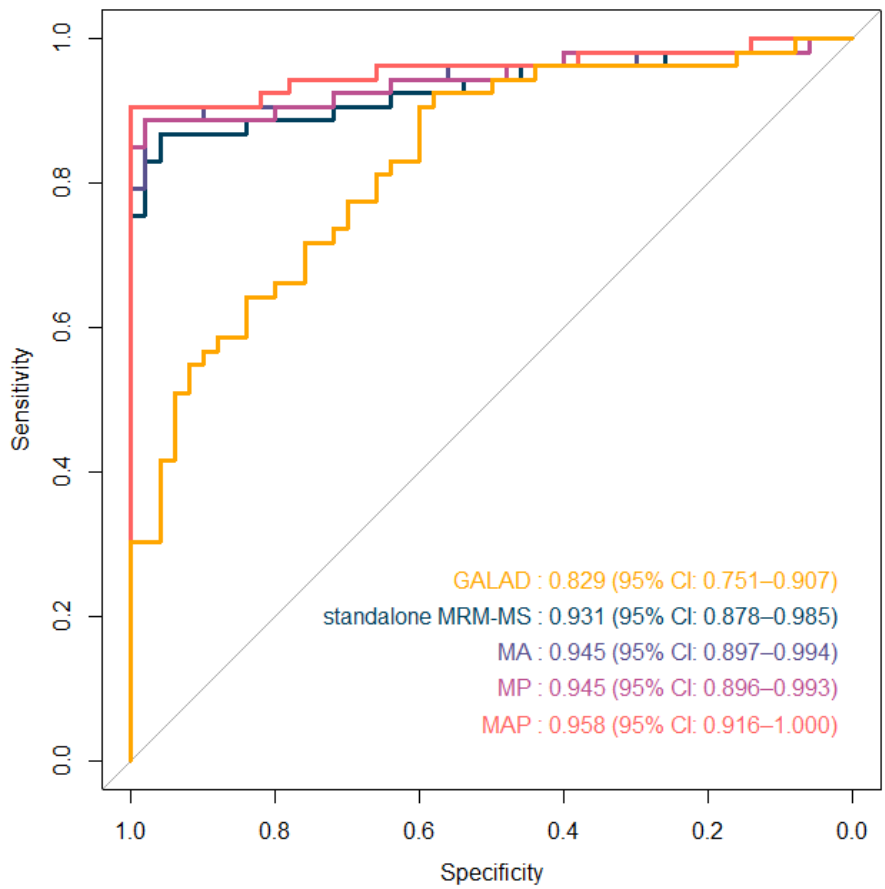

ROC curves of the GALAD score, standalone MRM-MS panel, MRM-MS + AFP (MA) panel, MRM-MS + PIVKA-II (MP) panel, and MRM-MS + AFP + PIVKA-II (MAP) panel in the GALAD cohort.

Table 1-6 Performance of AFP and the MRM-MS panel with and without AFP and PIVKA-II compared with GALAD in detecting HCC

	AUROC 95% CI	P value	Sensitivity (%)	Specificity (%)
GALAD	0.718 (0.751–0.907)		52.8	92.0
Standalone MRM-MS panel	0.931 (0.878–0.985)	<0.001*	88.7	82.0
MA panel	0.945 (0.897–0.994)	0.064†	92.5	70.0
MP panel	0.945 (0.896–0.993)	0.013†	88.7	98.0
MAP panel	0.958 (0.916–1.000)	0.009†	90.6	98.0

* AUROC of the standalone MRM-MS panel versus AUROC of GALAD score. † AUROC of the multimarker panel with AFP and/or PIVKA-II versus AUROC of the standalone MRM-MS panel. AUROC; area under the receiver operating characteristics curve; AFP, alpha-fetoprotein; MA, multiple reaction monitoring-mass spectrometer + AFP; MP, multiple reaction monitoring-mass spectrometer + protein induced by vitamin K absence or antagonist-II; MAP, multiple reaction monitoring-mass spectrometer + AFP + protein induced by vitamin K absence or antagonist-II.

1.3.5 Performance of the MRM-MS panel with and without AFP and PIVKA-II in detecting small (<2 cm) single HCC

Patients with small (ie, <2 cm) single HCC and high-risk controls in each set were analyzed. In the training set, the standalone MRM-MS panel had a significantly higher AUROC value (0.929 vs 0.775, P<0.001), greater sensitivity (76.6% vs 22.1%), and lower specificity (93.5% vs 97.5%) compared with AFP. The AUROC values of the MA (0.938; 95% CI, 0.909–0.968; P=0.072), MP (0.931; 95% CI, 0.898–0.963; P=0.498), and MAP panels (0.940; 95% CI, 0.911–0.969; P=0.074) were similar to that of the standalone MRM-MS panel. The sensitivity and specificity of the MAP panel were 72.7% and 96.5%, respectively. (Figure 1-4)

Figure 1-5 Performance of AFP and the MRM-MS panel with and without AFP and PIVKA-II in detecting small (<2 cm) single HCC

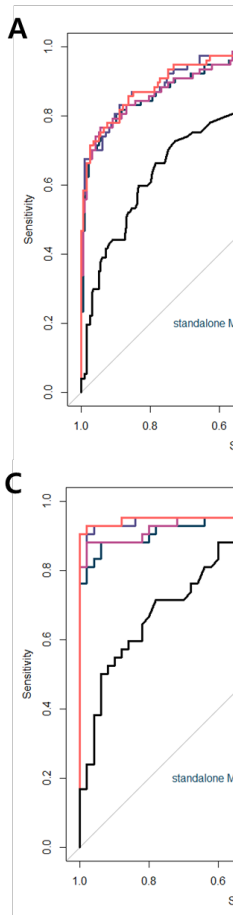

(A): ROC curve of AFP and the MRM-MS Panel with/without combination of AFP and/or PIVKA-II in the training set. (B): ROC curve of AFP and the MRM-MS Panel with/without combination of AFP and/or PIVKA-II in the test set. (C): ROC curve of AFP and the MRM-MS Panel with/without combination of AFP and/or PIVKA-II in the validation set.

In the test set, the MRM-MS panel yielded a significantly higher AUROC value (0.893 vs 0.593; P<0.001), better sensitivity (74.2% vs 22.6%), and lower specificity (81.2% vs 97.5%) than AFP. The AUROC values of the MA (0.895; 95% CI, 0.934–0.957; P=0.882), MP (0.893; 95% CI, 0.832–0.953; P=0.938), and MAP panels (0.894; 95% CI, 0.832–0.957; P=0.943) were comparable with that of the standalone MRM-MS panel. The sensitivity and specificity of the MAP panel were

77.4% and 82.4%, respectively.

In the validation set, the standalone MRM-MS panel had a significantly higher AUROC value (0.937 vs 0.806; P=0.019), greater sensitivity (88.1% vs 31.0%), and lower specificity (82.0% vs 96.0%) than AFP. The AUROC values of the MP (0.946; 95% CI, 0.892–1.000; P=0.04) and MAP panels (0.961; 95% CI, 0.912–1.000; P=0.026) were significantly higher versus the standalone MRM-MS panel, unlike the MA panel (0.955; 95% CI 0.901–1.000; P=0.062). The sensitivity and specificity of the MAP panel were 90.5% and 98.0%, respectively (Table 1-5).

Table 1-7 Performance of AFP and the MRM-MS panel with and without AFP and PIVKA-II in detecting small (<2 cm) single HCC

	AUROC 95% CI	P value	Sensitivity (%)	Specificity (%)
Training set				
AFP	0.775 (0.710–0.813)		22.1	97.5
Standalone MRM-MS panel	0.929 (0.896–0.962)	<0.001*	76.6	93.5
MA panel	0.938 (0.909–0.968)	0.072†	83.1	87.4
MP panel	0.931 (0.898–0.963)	0.498†	76.6	94.5
MAP panel	0.940 (0.911–0.969)	0.074†	72.7	96.5
Test set				
AFP	0.593 (0.464–0.721)		22.6	97.5
Standalone MRM-MS panel	0.893 (0.834–0.952)	<0.001*	74.2	81.2
MA panel	0.895 (0.834–0.957)	0.882†	90.3	74.1
MP panel	0.893 (0.832–0.953)	0.938†	74.2	78.8
MAP panel	0.894 (0.832–0.957)	0.943†	77.4	82.4
Validation set				
AFP	0.806 (0.717–0.896)		31.0	96.0
Standalone MRM-MS panel	0.937 (0.878–0.996)	0.019*	88.1	82.0
MA panel	0.955 (0.901–1.000)	0.062†	95.2	70.0
MP panel	0.946 (0.892–1.000)	0.040†	88.1	98.0
MAP panel	0.961 (0.912–1.000)	0.026†	90.5	98.0

* AUROC of the standalone MRM-MS panel versus AUROC of AFP. † AUROC of MA, MP, or MAP panel versus AUROC of the standalone MRM-MS panel. AUROC- area under the receiver operating characteristics curve; AFP- alpha-fetoprotein; MA- multiple reaction monitoring-mass spectrometer + AFP; MP- multiple reaction monitoring-mass spectrometer + protein induced by vitamin K absence or antagonist-II; MAP- multiple reaction monitoring-mass spectrometer + AFP + protein induced by vitamin K absence or antagonist-II.

1.3.6 Subgroup analysis

A separate subgroup analysis was performed for patients with cirrhosis in each set and those with noncirrhotic CHB in the training and test sets. An analysis of participants with noncirrhotic CHB in the validation set was not feasible, because all controls in the set had cirrhosis.

For patients with cirrhosis, the standalone MRM-MS model yielded a significantly higher AUROC value (0.927 vs 0.790; P<0.001), higher sensitivity (76.6% vs 20.2%), and lower specificity (94.9% vs 97.5%) than AFP in the training set. The AUROC value of MAP panel (0.945; 95% CI, 0.919–0.970; P=0.021) was significantly higher versus the standalone MRM-MS panel. In the test and validation sets, the MRM-MS model also had a significantly higher AUROC value (0.875 and 0.944 vs 0.712 and 0.798; P=0.005 and P<0.001, respectively), greater sensitivity (76.8% and 88.9% vs 28.6% and 36.7%, respectively), and lower specificity (78.1% and 82.0% vs 96.9% and 96.0%, respectively) than AFP alone. The AUROC value of the MRM-MS panel improved with the addition of AFP and PIVKA-II (ie, MAP panel) in the validation set (0.973; 95% CI, 0.949–0.997; P=0.001), but this increase was not significant in the test set (0.897; 95% CI, 0.839–0.954; P=0.303) (Table 1-8 and Figure 1-6).

Table 1-8 Subgroup analysis of patients with cirrhosis

	AUROC 95% CI	P value	Sensitivity (%)	Specificity (%)
Training set				
AFP	0.790 (0.736–0.844)		20.2	97.5
Standalone MRM-MS panel	0.927 (0.898–0.957)	<0.001*	76.6	94.9
MA panel	0.944 (0.919–0.969)	0.019†	86.3	87.9
MP panel	0.928 (0.899–0.958)	0.672†	76.6	95.5
MAP panel	0.945 (0.919–0.970)	0.021†	77.4	96.2
Test set				
AFP	0.712 (0.617–0.807)		28.6	96.9
Standalone MRM-MS panel	0.875 (0.815–0.937)	0.005*	76.8	78.1
MA panel	0.885 (0.825–0.945)	0.591†	87.5	70.3
MP panel	0.890 (0.833–0.947)	0.088†	80.4	76.6
MAP panel	0.897 (0.839–0.954)	0.303†	80.4	81.3
Validation set				
AFP	0.798 (0.725–0.872)		36.7	96.0
Standalone MRM-MS panel	0.944 (0.909–0.980)	<0.001*	88.9	82.0
MA panel	0.960 (0.930–0.990)	0.005†	92.2	70.0
MP panel	0.956 (0.924–0.987)	0.005†	88.9	98.0
MAP panel	0.973 (0.949–0.997)	0.001†	90.0	98.0

* AUROC of standalone MRM-MS panel versus AUROC of AFP. † AUROC of multimarker panel with AFP and/or PIVKA-II versus AUROC of the standalone MRM-MS panel. AUROC; area under the receiver operating characteristics curve; AFP, alpha-fetoprotein; MA, multiple reaction monitoring-mass spectrometer + AFP; MP, multiple reaction monitoring-mass spectrometer + protein induced by vitamin K absence or antagonist-II; MAP, multiple reaction monitoring-mass spectrometer + AFP + protein induced by vitamin K absence or antagonist-II.

For patients with noncirrhotic CHB in the training set, the MRM-MS panel had a significantly higher AUROC value (0.951 vs 0.734; P<0.001), greater sensitivity (86.2% vs 13.8%), and lower specificity (85.3% vs 97.1%) than AFP, whereas the MAP panel had a statistically similar AUROC value (0.962; 95% CI, 0.929–0.994; P=0.111) as the standalone MRM-MS panel. In the test set, the MRM-MS panel also had a significantly higher AUROC value (0.909 vs 0.702; P<0.001) compared with AFP alone, and the addition of AFP and PIVKA-II (ie, the MAP panel) did not significantly improve the AUROC value (0.931; 95% CI, 0.854–1.000; P=0.298) (Table 1-9 and Figure 1-6).

Table 1-9 Subgroup analysis of patients with chronic hepatitis B

	AUROC 95% CI	P value	Sensitivity (%)	Specificity (%)
Training set				
AFP	0.734 (0.633–0.836)		13.8	97.1
Standalone MRM-MS panel	0.951 (0.909–0.992)	<0.001*	86.2	85.3
MA panel	0.955 (0.918–0.993)	0.286†	92.3	85.3
MP panel	0.958 (0.923–0.994)	0.085†	87.7	88.2
MAP panel	0.962 (0.929–0.994)	0.111†	84.6	97.1
Test set				
AFP	0.702 (0.525–0.878)		15.0	100.0
Standalone MRM-MS panel	0.909 (0.813–1.000)	0.048*	85.0	87.5
MA panel	0.922 (0.838–1.000)	0.388†	90.0	81.3
MP panel	0.913 (0.822–1.000)	0.843†	85.0	81.3
MAP panel	0.931 (0.854–1.000)	0.298†	85.0	81.3

* AUROC of the standalone MRM-MS panel versus AUROC of AFP. † AUROC of multimarker panel with AFP and/or PIVKA-II versus AUROC of the standalone MRM-MS panel. AUROC; area under the receiver operating characteristics curve; AFP, alpha-fetoprotein; MA, multiple reaction monitoring-mass spectrometer + AFP; MP, multiple reaction monitoring-mass spectrometer + protein induced by vitamin K absence or antagonist-II; MAP, multiple reaction monitoring-mass spectrometer + AFP + protein induced by vitamin K absence or antagonist-II.

Figure 1-6 Subgroup analysis of patients with cirrhosis and chronic hepatitis B

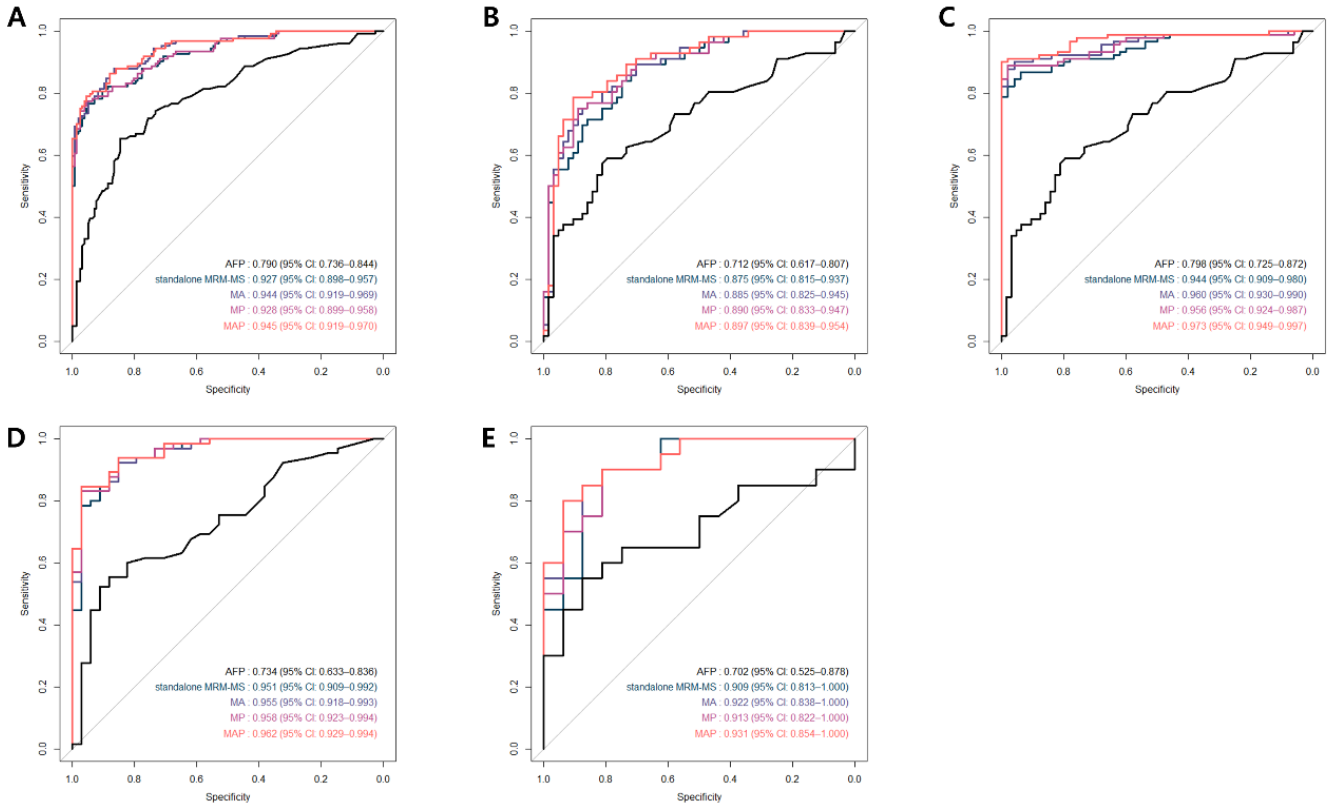

ROC curves of AFP, standalone MRM-MS panel, MRM-MS + AFP (MA) panel, MRM-MS + PIVKA-II (MP) panel, and MRM-MS + AFP + PIVKA-II (MAP) panel in the (A) training set, (B) test set, and (C) validation set with cirrhosis and in the (D) training set and (E) test set with chronic hepatitis B.

1.4. Discussion

We have developed a multimarker panel of 17 proteins by MRM-MS analysis for detecting HCC. This MRM-MS panel performed significantly better than AFP in differentiating HCC patients from controls in every dataset, especially with regard to sensitivity. The incorporation of AFP and PIVKA-II into the MRM-MS panel improved its performance in every set, although statistical significance was not achieved with the test set. The diagnostic superiority of the MRM-MS panel over AFP was maintained in patients with small single HCC, but the significant improvement that was affected by the addition of AFP and PIVKA-II was observed only in the validation set.

With the limitation of sample yield, only a small portion of the cohort could have analyzed and validated. Nonetheless, the MRM-MS panel outperformed the GALAD score and demonstrated its efficacy in identifying HCC patients among cirrhotic patients and those with noncirrhotic CHB. We hope the performance of the panel and the GALAD score comparison can be validated in other study.

The low concentrations of potential biomarkers and the wide range of protein levels are major setbacks in the proteomic analysis of serum(32). MRM-MS, which can detect attomole levels of peptides(33-36) and quantify hundreds of peptides in an automated manner(37, 38), is an effective modality in examining and validating candidate biomarkers for early detection of HCC. The data that are generated by MRM-MS assays are highly reproducible(39).

HCC surveillance programs that are based on abdominal ultrasonography with and without serum AFP assay have low sensitivities in cirrhotic patients(12, 40),

whose alterations in liver parenchyma are associated with poor imaging quality(41) and a high risk of HCC(42). Although recent studies have examined the value of cross-sectional imaging modalities (eg, computed tomography and magnetic resonance imaging) as potential alternatives(43-45), their limited accessibility and high cost are major barriers to their widespread use(46). HCC surveillance using an MRM-MS panel has the advantages of being readily available and cost-effective, because it requires only blood samples for mass spectrometry assays.

No study that has aimed to identify new HCC serum markers through mass spectrometry(47-51) has validated the discriminatory performance of the identified markers in a chronologically separately collected, multicenter cohort. The current study is also distinct from a previous report by our group(27), in that data preprocessing was adopted before the selection of the markers and that fewer markers were involved in the developed panel. The smaller number of markers renders the MRM-MS panel economically competitive with regard to the amount of internal standard peptides and reagents that are needed for mass spectrometry assays(52).

Our MRM-MS panel showed excellent accuracy in discriminating HCC patients, with an AUROC value of 0.891 being the lowest across all analyses, considering that a value over 0.8 is excellent(53). However, its specificity was lower than that of AFP, as was the case with our group's earlier panel. AFP, despite its low sensitivity of 39% to 65% in detecting HCC(54), improved the sensitivity when added to the MRM-MS panel, although its specificity declined. This drawback was overcome by introducing PIVKA-II, which is more specific than AFP in detecting HCC(55). A similar trend was observed when the analysis was confined to patients with small single HCC. These results imply that the serum

levels of proteins in the MRM-MS panel are affected by the presence of HCC through mechanisms that are independent of those that affect the levels of AFP and PIVKA-II. Notably, the MRM-MS panel was consistently reliable when classifying patients with cirrhosis and those with noncirrhotic CHB, in contrast to AFP, the levels of are frequently elevated in patients with cirrhosis or CHB(56).

Among 17 proteins in the marker, several markers have been reported directly associated with HCC. SERPINC1 is considered as one of the most important serine protease inhibitors in plasma that regulates the blood coagulation cascade. This surrogate protein was reported being associated independently with HCC, consistent with a previous report(57, 58). MCAM promotes tumor growth, angiogenesis and metastasis and is regarded as a promising target for tumor therapy(59). This protein was observed highly elevated in HCC patients(60). The expression of AMBP has been found to be down-regulated in both HCC tissues and cell lines(58). THBS1 is linked to tumor invasiveness and progression in HCC and is a proangiogenic factor that stimulates angiogenesis in HCC(61). LCAT has been shown to generate cholesteryl esters (CEs) in the circulation of males from high-density lipoprotein (HDL) and transfer them to apolipoprotein (apo) B-containing lipoproteins with the help of lipid transfer protein (LTP)(62). A previous research has purpose using LCAT as diagnostic model for HCC(63). C1QC associates with the proenzymes C1r and C1s to yield C1, the first component of the serum complement system. In a previous study, upregulation of C1QC was reported in HCC cases(64). Both complement components have been reported associated with HCC. As an important part of the complement system, C2 is mainly involved in the formation of C3 convertase of the classical pathway and MBL pathway. Single nucleotide polymorphism (SNP) of C2 was first found to be related with systemic

lupus erythematosus and age-related macular degeneration(65, 66). complement component 2 (C2) to be associated with CHB by exome sequencing(67). A C6 is an indispensable ingredient for MAC formation in complement defense against invading pathogens, which has also been reported to be associated with HCC(68). APOH is a multifunctional apolipoprotein encoded by the human APOH gene and one of its functions is to bind cardiolipin(69). APOH was highly overexpressed in hepatitis B-related HCC tissue(70).

Although haven't been reported associated directly with HCC, other proteins showed statistically significant attribute to the model. PPBP is a protein that is released in large amounts from platelets following their activation(71). It stimulates various processes including mitogenesis, synthesis of extracellular matrix, glucose metabolism and synthesis of plasminogen activator(72, 73). cytoskeletal proteins CFL1 an actin depolymerizing protein involved in invadopodium formation and required for tumor cell directionality in response to chemotactic or growth-factor stimulation(74, 75). C4A is a blood coagulation protein reported to fluctuate in lupus nephritis which are related to colorectal cancer development(76). UCHL3 displays hydrolyzing activity during the processing of both ubiquitin precursors and the poly-Ub chain from substrates(77, 78). Moreover, UCHL3 cleaves Nedd8, a ubiquitin-like protein, from substrates, which is a unique feature of this enzyme(79, 80). CNDP1 is a secreted protein of 57 kDa found in human blood and the central nervous system, which act as homodimer(81). The carbonic anhydrase family (CAHs) plays an important role in extracellular acidification; a possible involvement CA2 in tumor invasion has been proposed(82). SAA4 exists as a minor apolipoprotein on high-density lipoprotein in plasma and is a minor acute-phase reactant in humans. SAA4 can be used as a possible nutritional marker of

hepatic protein synthesis in the absence of inflammation(83). SERPINA10 was reported to be associated with tumor progression(84).

Our study has several limitations. The depletion of the 6 most abundant proteins before the MRM-MS assays might have eliminated other proteins with significant discriminatory value, as inferred from the finding that AFP was not included in the list of the 17 markers. This issue has been discussed in other proteomic studies(85, 86) and was addressed in our study through the subsequent addition of AFP, which is the only commonly used serum biomarker for screening HCC(54).

Further, it is unknown whether the MRM-MS panel is useful for patients with other risk factors for HCC, such as alcoholic liver cirrhosis, or nonalcoholic fatty liver disease. However, most cases of HCC are associated with cirrhosis that is related to CHB or CHC(87); thus, our study population represents most patients who are subject to an HCC screen. Also, the effectiveness of the MRM-MS panel in patients of various ethnicities is unverified—all of our participants were Korean. Finally, no comparison with abdominal ultrasonography was performed in this study.

Increased AUROC value in independent validation cohort to the derivation cohort were reported among all the performance comparison in the result. Not only the panel itself but AUROC of AFP also was increased. This phenomenon could be explained as error rates presented by the sample size of validation cohort, which all the AUROC of the model combinations and AFP were within 95% CI of the corresponding training set AUROC(88).

1.5. Conclusion

In conclusion, with chronically separated cohort, this MRM-MS multimarker panel, comprising 17 proteins, showed excellent performance in distinguishing HCC patients from high-risk controls with cirrhosis or CHB or CHC despite the collection time. Its combination with AFP and PIVKA-II enhanced its performance, although statistical significance was not consistently reached. Prospective studies are warranted to determine whether our MRM-MS panel is a viable alternative to abdominal ultrasonography in HCC surveillance.

Chapter 2.

Panel Development Software for biomarker Study

2.1. Introduction

Biomarkers are instrumental in the detection and management of diseases(89). Despite an enormous number of publications, novel technologies, and abundant funding, very few biomarkers make it to clinical practice. These phenomena can be partially attributed to the lack of a clear and accessible path for selection of biomarker and validating biomarker candidates for clinical use(90).

A clinically applicable marker panel requires various computational methods in panel development and proving clinical level reproducibility. Machine Learning Algorithms are frequently proposed for Multi marker panel development along with data preprocess methods for statistically accurate analysis.

Because biomarkers vary in characteristics and are evaluated accordingly, it is necessary to validate biomarker assays by several criteria and methods(91, 92). For instance, blood protein-based biomarkers are often detected using quantitative immunoassays. In contrast, protein-based biomarkers and DNA-based biomarkers in tissue are generally detected using immunohistochemical and in situ hybridization assays, respectively(93). In the past decade, mRNA-based biomarkers have been studied using microarrays(94).

Regardless of the assay type, a biomarker assay must be analytically validated prior to clinical use. Analytical method validation involves confirming the accuracy, precision, specificity, robustness, and stability of the biomarker assay and overall method(91, 92, 95-97) Other assay validation criteria include linearity, parallelism, recovery following analyte addition, and functional sensitivity.

Multiple reaction monitoring-mass spectrometry (MRM-MS) assays are

suitable for measuring multi-marker panels in clinical applications(98-101). An MRM-MS assay can accurately quantify multiple biomarkers. However, the panel development and analytical validation of MRM-MS assays, which simultaneously measure thousands of transitions corresponding to quantitative values of multi-markers, can be rather difficult and laborious, especially if the interpretation and evaluation of numerous procedures and categories are performed manually.

Currently, MRM-MS data can be processed in part using vendor-specific software (e.g., MassHunter Quantitative Analysis, Agilent; MultiQuant, ABSciex; Pinpoint, Thermo Scientific) or vendor-independent programs, such as Skyline(102-105). Overall, these software programs are generally used to perform a preliminary analysis of mass spectral data and transitions and also allow the user to verify and edit peak selection/integration. None of these software programs possess a feature that gives insight into the marker panel development and analytical validation of detected transitions of a given MRM-MS assay.

For MRM-MS assay to be more accessible in the clinical area, the assay requires a linear process of multi biomarker panel development and analytical validation process to be used for measuring multiple biomarkers in clinical settings. However, limitations in the analytical validation of the MRM-MS assay will be encountered. To address this challenge, we developed and launched two web application: WMD (Web Model Developer) for panel development and an assay portal, named M-MVP (MRM–MS assay-analytical method Validation Portal, http://pnbvalid.snu.ac.kr), as a free tool (Figure 1). WMD is a python-based web application that assists preliminary marker panel development with basic machine learning functions while M-MVP is designed to automatically evaluate MRM-MS assay data. The method validation items configured in M-MVP are designed to

meet the requirements of three sets of guidelines [US Food and Drug Administration (FDA), European Medicines Agency (EMA), and Korea Food and Drug Administration (KFDA)].

Various Panel development and analytical validation procedures can be evaluated with both web application with minimal effort. While WMD process quantified candidate biomarker data and develop multimarker panel, M-MVP centralizes all method validation calculations, which significantly reduces the time, effort, and errors that would likely occur with manual processing. These advantages facilitate the implementation of MRM-MS assays in clinical settings by simplifying the analytical validation computational process of multi-marker panel assays.

2.2. Methods

2.2.1 Architecture of WMD

To implant dominantly used machine learning module in web application, Python(106) were used as basic programming language while the web application was structured using Django framework (Django Software Foundation. Django [Internet]. 2019. Available from: https://djangoproject.com). Django framework enabled developing secured and maintainable website with minimum effort and focus on development of core function. Pandas(107) module was implanted for data loading and reconstruction.

Data manipulation as data normalization prior to feature selection is an essential procedure for machine to study the data without biased abnormality(108). In WMD, we provide two functions commonly used in biology data study: batch effect correction and data transformation.

Batch effect is a phenomenon observed in biological study which non-biological differences that make samples in different batches not directly comparable(109). If not corrected properly, the data might lead to biased biological insight. Several statistical methods and programming library have been introduced to correct such effects(110). In this web application, we implanted pyComBat module(111) which utilized Empirical Bayes method to normalize batch effect(112).

Data transformation was performed by comparing skewness of every independent feature within dataset with normal, log, square, and square root form(113). Each feature in the dataset are transformed with NumPy(114) to each form and absolute z score of each group, case and control cohort, are calculated

and added. Finally, the data set are transformed into the form with lowest absolute z score.

Prior to feature selection, reducing statistically insignificant features are encouraged. In this web application, Students' T-test and individual AUROC calculation and cut-off customization are provided. P value of Students' T-test and AUROC are calculated by SciPy(115) and Scikit-learn(116) module, respectively.

Feature selection methods were provided with 3 options: Forward, Backward and Recursive Feature Elimination which are all wrapper methods-based. In wrapper methods, the feature selection process is based on a specific machine learning algorithm that we are trying to fit on a given dataset. It follows a greedy search approach by evaluating all the possible combinations of features against the evaluation criterion. The evaluation criterion is simply the performance measure which depends on the type of problem, for e.g. For regression evaluation criterion can be p-values, R-squared, Adjusted R-squared, similarly for classification the evaluation criterion can be accuracy, precision, recall, f1-score, etc. Finally, it selects the combination of features that gives the optimal results for the specified machine learning algorithm. When testing an estimator or setting hyperparameters, one needs a reliable metric to evaluate its performance. Using the same data for training and testing is not acceptable because it leads to overly confident model performance, a phenomenon also known as overfitting. Cross-validation is a technique that allows one to reliably evaluate an estimator on a given dataset. It consists in iteratively fitting the estimator on a fraction of the data, called training set, and testing it on the left-out unseen data, called test set. Several strategies exist to partition the data. For example, k-fold cross-validation consists in dividing (randomly or not) the samples in k subsets: each subset is then used once as testing

set while the others k − 1 subsets are used to train the estimator. This is one of the simplest and most widely used cross-validation strategies. In this application, we provide 3- or 5-fold cross-validation.

Logistic Regression (LR) or Support Vector Machine (SVM) are selectable as classifier with hyperparameter tuning options. Hyperparameter tuning is the problem of choosing a set of optimal hyperparameters for a learning algorithm. Although tuning hyperparameter may lead to optimum results from the dataset, it requires certain level of understanding to machine learning algorithm. WMD was developed for researcher who are not familiar with implanting machine learning techniques to a biomarker study and collect a preliminary result from the dataset. Nonetheless, including parameter tuning options for advanced researcher would results in a more optimum result for user. 15 parameter options for LR and 13 parameter options for SVM are provided by scikit-learn package.

In scikit-learn, all objects and algorithms accept input data in the form of 2-dimensional arrays of size samples × features. For this web application, uploaded data need to upload quantified MS data as such.

2.2.2 Architecture of M-MVP

The SPRING(117) framework, which features a standard Model-View-Controller (MVC) ideal for webserver applications, was the fundamental component of the server that formed M-MVP's infrastructure. As part of the MVC model, the Java(118) controller handles requests and mapping, in which JavaScript(119) works as a dynamic web page, with Ajax(120) for asynchronous web applications and file upload for user interfaces. Mybatis (Mybatis. Mybatis

[Internet]. 2004. Available from: https://www.mybatis.org) framework was used to handle Structured Query Language (SQL) statements for data calculation and storage to the MySQL(121) Database Server. Bootstrap (Bootstrap. Bootstrap [Internet]. 2011. Available from: https://www.getboostrap.com) is a general open source jQuery(jQuery. jQuery [Internet]. 2006. Available from: https://jquery.com) library for web page user interface design. Bootstrap was used to design the table format in M-MVP that was used for cases in which evaluation guidelines and output files were presented in table form. Gradle(122) is a build automation system that automatically manages libraries and builds a Web Application Archive (WAR) file that is deployed on a Tomcat server(The Apache Software Foundation. Tomcat [Internet]. 1999. Available from: https://tomcat.apache.org/). Because floating-point calculation varies by programming language, data calculation and validation were performed exclusively with SQL query to ensure consistency.

To specify the architecture of the portal, Controllers, which are the main java files that control all the input output commands, are divided into three categories. LoginController.java handles login related request from the client, where InfoController.java handles experiment data information of the logged in user. All other request for webpage loading or calculation functions are handled in SampleController.java. Upload and calculation of user data requires server to connect with the database server, which are controlled by Mybatis package. Within the package xml files contains SQL queries, which are called by the controller under user's request. The database contains individual schema for user information, experimental information and uploaded data. All the webpages are composed with JSP, where design is composed with html and CSS. Dynatable(Alpha Jango. Dynatable [Internet]. 2014. Available from: https://www.dynatable.com/), an open

source interactive table using jQuery is implanted for the entire table format of the portal.

2.2.2.1 Data format

Depending on the analyte and the type of mass spectrometer, data analysis software may vary. Skyline (MacCoss Lab) is the most commonly used data processing software for MRM-MS. We developed M-MVP to accept Skyline output files in csv format, in which the column and analyte names must agree with our specified format. We defined validation categories, such as calibration curve, specificity, sensitivity, carryover, precision, accuracy, matrix effects, recovery, dilution integrity, stability, and QC (samples and frequency), based on guidelines from the FDA, EMA, and KFDA. For all validation categories, step-by-step instructions for adopting the Skyline output file into the format that M-MVP requires are provided. Only with a specific format can M-MVP accept the uploaded Skyline data for calculations and validation.

To develop the portal, we used the entire validation datasets of our previous study(123). The datasets were verified to pass the standards of all 3 administrations.

2.2.2.2 Calculation and Validation Method

For calculations, M-MVP extracts light and heavy area values from the Skyline files. PAR and concentration ratio (from the reverse calibration curve data) are used for linear regression analysis. The user chooses a linear equation that is used by M-MVP to calculate the concentrations of subsequent categories, such as

Sensitivity and Recovery. For some categories, the standard deviation and coefficient of variation (CV) of PAR or concentration are calculated. Percent difference between the initial value and measured value is also calculated when required by the guidelines.

The calibration curve presents reverse and forward calibration curve data. The calibration curve falls within the range of measured concentrations by the instrument in which mass spectrometry can show linear measurements. Specificity is assessed by definite signals of analyte and Internal Standard (IS) in blank samples. Sensitivity is assessed by the first calibrator or lower limit of quantification (LLOQ), when the method provides acceptable precision and accuracy. Evaluation of carryover is assessed by injecting blank samples following a high-concentration sample or samples that are used for upper limit of quantification (ULOQ). Precision and accuracy are assessed by analyzing QC samples. Within-run precision and accuracy are calculated by averaging the concentration of replicates of each target QC concentration on each day, whereas between-run precision and accuracy are calculated by averaging the first run of each target QC concentration across all days. Accuracy values are assessed by dividing the measured concentration by the expected concentration.

For the validation of matrix effects, PAR of a spiked target in each matrix and in neat solution is calculated, and then, the values of all six matrices at the same concentration are averaged. Recovery was assessed as the relative recovery of recovered target to input target in terms of PAR at each QC concentration. Dilution integrity evaluates whether dilution affects the precision and accuracy and is assessed by calculating the change in concentration resulting from sample dilution. For stability validation, M-MVP sets day-0 as the standard point and compares the

measured values at day-0 with other conditions at every QC concentration. In terms of QC (samples and frequency), the accuracy of QC samples is assessed in at least 5% of the total number of patient samples. This method assures that sample preparation and storage do not affect sample concentration. All aforementioned calculations are performed by SQL queries in the MySQL server; calculation methods are summarized in Table 2-1. M-MVP provides an assorted list of validation standards that are issued by the three regulatory agencies as references from FDA (https://www.fda.gov/media/70858/download), EMA (https://www.ema.europa.eu/en/documents/scientific-guideline/guideline-bioanalytical-method-validation_en.pdf), and kFDA (https://www.spmed.kr/bbs/bbs_download.php?idx=74&download=1).

Table 2-1 Specific value description and formula for the 11 categories

No.	Category	Values	Explanation
1	Calibration Curve	Signal to Noise	$\frac{\text{PAR } calibrator}{\text{PAR } zero\ sample}$
		Bias	$\frac{\text{Slope of each matrix} - \text{Mean slope}}{\text{Mean slope}} \times 100$
2	Specificity	Interference (%)	$\frac{\text{Peak Area } blank\ sample}{\text{Peak Area } calibrator\ 1} \times 100$
3	Sensitivity	Signal to Noise	$\frac{\text{PAR } calibrator\ 1}{\text{PAR } zero\ sample}$
		Precision	CV of calibrator 1
		Accuracy	$\frac{\text{Measured concentration}}{\text{Expected concentration}} \times 100$
4	Carryover	Carryover	$\frac{\text{Peak Area } blank\ sample}{\text{Peak Area } calibrator\ 1} \times 100$
5,6	Precision & Accuracy	Intra-Day CV	Averaging the mean values of the each replicates on each day
		Inter-Day CV	Averaging the first replicate of each day
		Recovery	measured concentration/expected concentration × 100
		Total CV	$\sqrt{CVinter^2 + CVintra^2}$
7	Matrix Effect	Matrix Effect	$\frac{\text{Serum matrix}}{\text{Buffer matrix}} \times 100$
8	Recovery	Recovery	$\frac{\text{Matrix spiked into serum at the beginning of assay}}{\text{Matrix spiked during the elution step}} \times 100$
9	Dilution Integrity	Accuracy	
10	Stability	Recovery	$\frac{\text{Concentration}}{0 - \text{day Concentration}} \times 100$
11	QC (samples and frequency)	Accuracy	$\frac{\text{Measured concentration}}{\text{Expected concentration}} \times 100$

2.2.2.3 Implementation

A schematic of the M-MVP pipeline is shown in (Figure 2). The user is required to log in as a guest or with the registered ID and password that are issued by the administrator. The process for the analytical method validation is accessible from the validation tab on the main page of M-MVP (Figure 1). On the following page, users are required to input information regarding their experiment and corresponding validated data. Once the user provides all required fields, a unique ID of the experiment is generated and is applied by the user to access and proceed with uploading the data. We designed the portal with a login function for two critical obstacles when evaluating the method: to avoid uploading the same files each session if the user did not pass the designated criteria in the first attempt and to manage each distinct experiment easily under the designated login ID. We also developed a guest log-in feature that does not require a login that features a nearly identical login process that differs by requiring users to remember their experiment ID. Uploaded data are stored and deleted after 1 week from the initial upload.

To proceed to the validation step, users operate three separate tasks. Users must upload all experimental data that are relevant to each of the 11 categories; two entries for calibration curve are available for upload. Only the categories with uploaded files will be validated according to integrative multinational guidelines. Although multiple data files for each category can be uploaded, only the most recently uploaded files are used for calculations and validation. This design allows users to re-do one specific category, as opposed to repeating the entire experiment. The next step is to upload the expected concentrations. Accuracy is defined as the closeness of agreement between an assay result (experimental measurement) and

the expected concentration (true value). With respect to accuracy measurements, users must input true values for calibration curve, quality control (QC), and dilution integrity in the corresponding web page of M-MVP so that calculations and validation are performed. The last step is for the user to choose the scale of the calibration curve, which is subsequently reflected in the corresponding calculations of the other categories. Under the Data menu, the “Linear Regression” page contains the linearity result for each transition (Figure 6). The user is given an option to choose normal, log2, or log10 scale for calculating the concentration. Once the user chooses a scale, the result is shown instantly in table form. By showing the intercepts, slope, and R2 in a table, M-MVP provides flexibility to the user for determining which one should be used to calculate the linear regression. The linear equation that the user selects from the Reverse Calibration Curve page is used for calculating the concentration of other categories. With all steps accomplished, M-MVP processes the calculation and method evaluation and shows the results to the user.

2.3. Result

2.3.1 Web Model Developer

The main objective of WMD is to suggest potential combination of biomarker and provide performance of the combination visually. The web application provides essential statistical computational function for biomarker study within one web page divided in 3 sections: Data-preprocess, Feature Selection and Predict page.

In the Data-preprocess section, the application provides 3 core data process function prior to data analysis (Figure 2-1). Batch effect correction is the procedure of removing variability from your data that is not due to your variable of interest. Batch effects are due to technical differences between your samples, such as the type of sequencing machine or even the technician that ran the sample. To perform batch correction, uploaded data must include batch number of each sample data with other variance. To provide visualized image of batch effect correction, WMD also displays before and after box chart of the uploaded data manipulated by batch effect correction (Figure 2-2). In a separate tab only for batch effect correction inspection, user can discover distribution of data before and after batch effect correction. Outlier values are displayed as dots in the figure.

The goal of normalization is to transform features to be on a similar scale which improves the performance and training stability of the model. In the application, we provide data transformation based on skewness of each feature in the data. Calculation Z-score of each feature with method selected, which are Square, Square Root and Logarithm to normal scale, the application will transform

each feature with the best way of normalizing the data. In many data analysis study, if only prepared with one large dataset, separation of the dataset into train and test set are required for validation of the study. In this application we provide data split function with selectable split ratio of the data. Selecting the function in need and uploading the raw data, the web application will process and provide the data to download, where one csv data will be provided if data divide function is not selected, train and test data if selected.

Figure 2-1 Data-Preprocess page

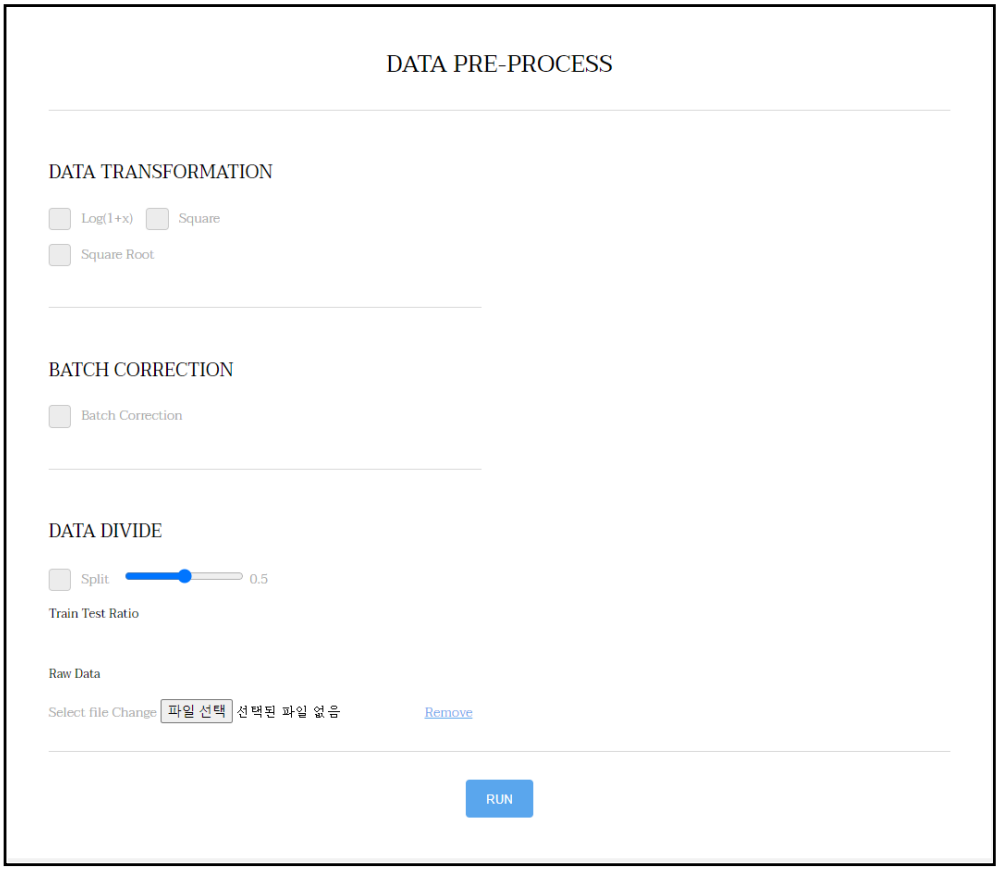

Figure 2-2 Box plot function for Batch Effect Correction

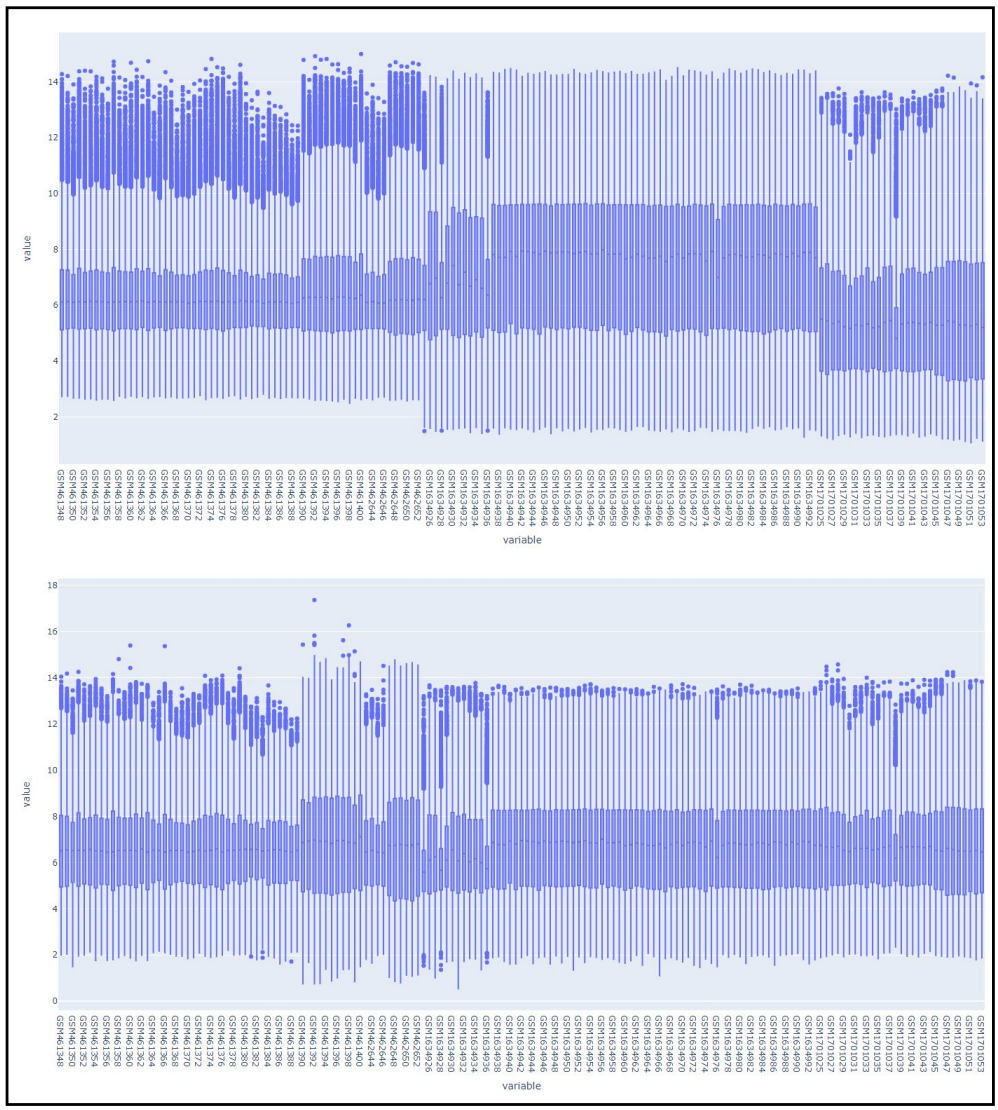

Whether process the data prior to feature selection or not, the Feature Selection Section of the application can proceed with its core function (Figure 2-3). In general, all the features provided in the data will be tested for feature candidate. For machine to select statistically significant candidates within the data, the application provides a pre-feature selection base on p-value of Student's T-test and AUROC value of the individual candidates. If chosen, the features in the data

under conditions selected by the researcher, for example p-value under 0.05 and AUROC more than 0.6, will be processed with feature selection. In this application, Forward, Backward selection and Recursive Feature Elimination (RFE) which are all wrapper methods-based technique are provided. After selection the selection methods, user have to choose which estimator, provided Logistic regression and SVM, to analysis the best features to represent the data. User can also choose to perform 3- or 5-fold cross validation with maximum of 10 repetition to aim for a more statistically general feature combination. WMD provides LR and SVM for classifier, with hyperparameter tuning options (Figure 2-4). Without editing hyperparameter, WMD will process with default setting. When data are uploaded and processed, the web application will the best set of features below the “Run” button as text separated with comma.

Figure 2-3 Feature Selection Page

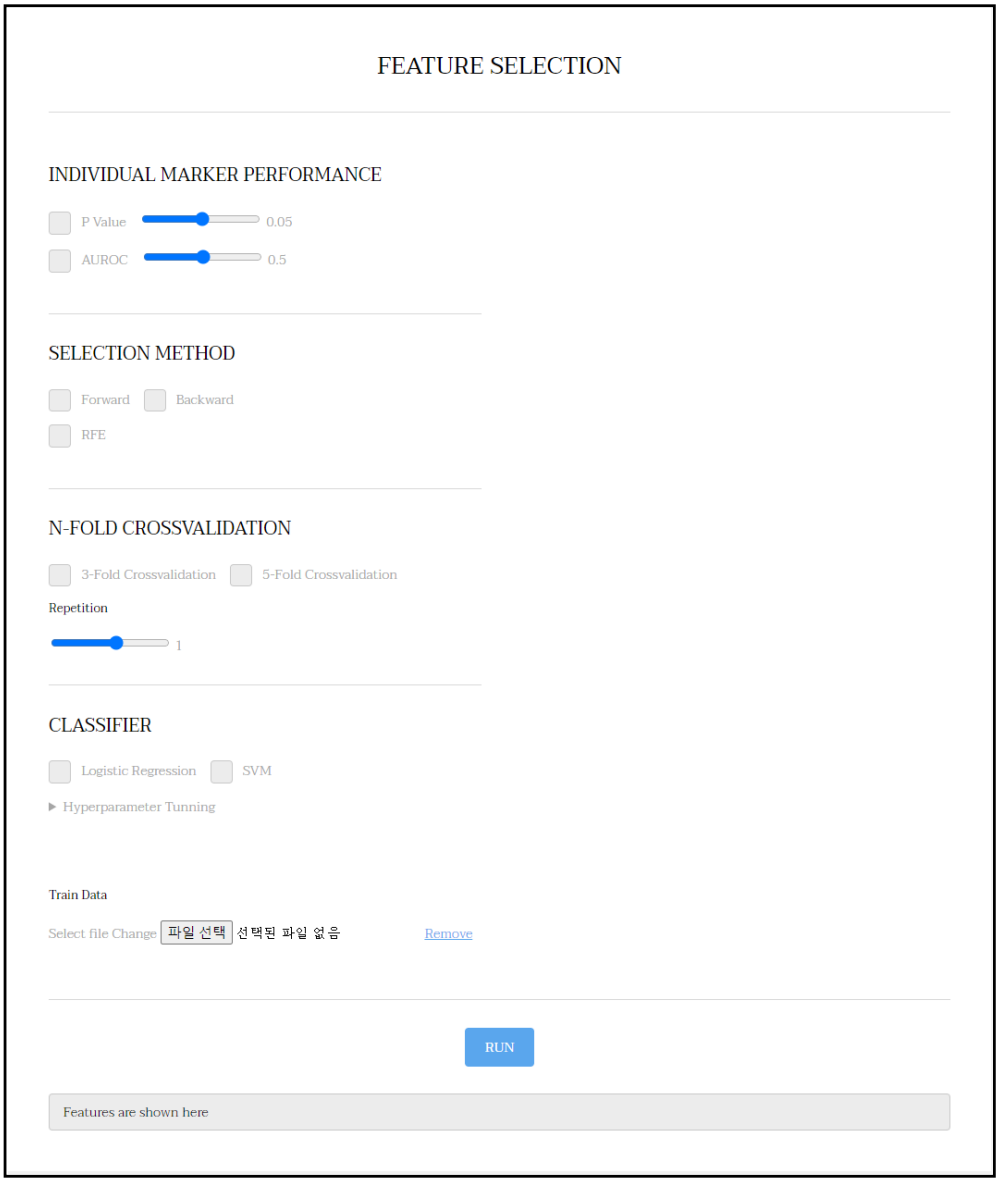

Figure 2-4 Classifier Hyperparameter Tuning

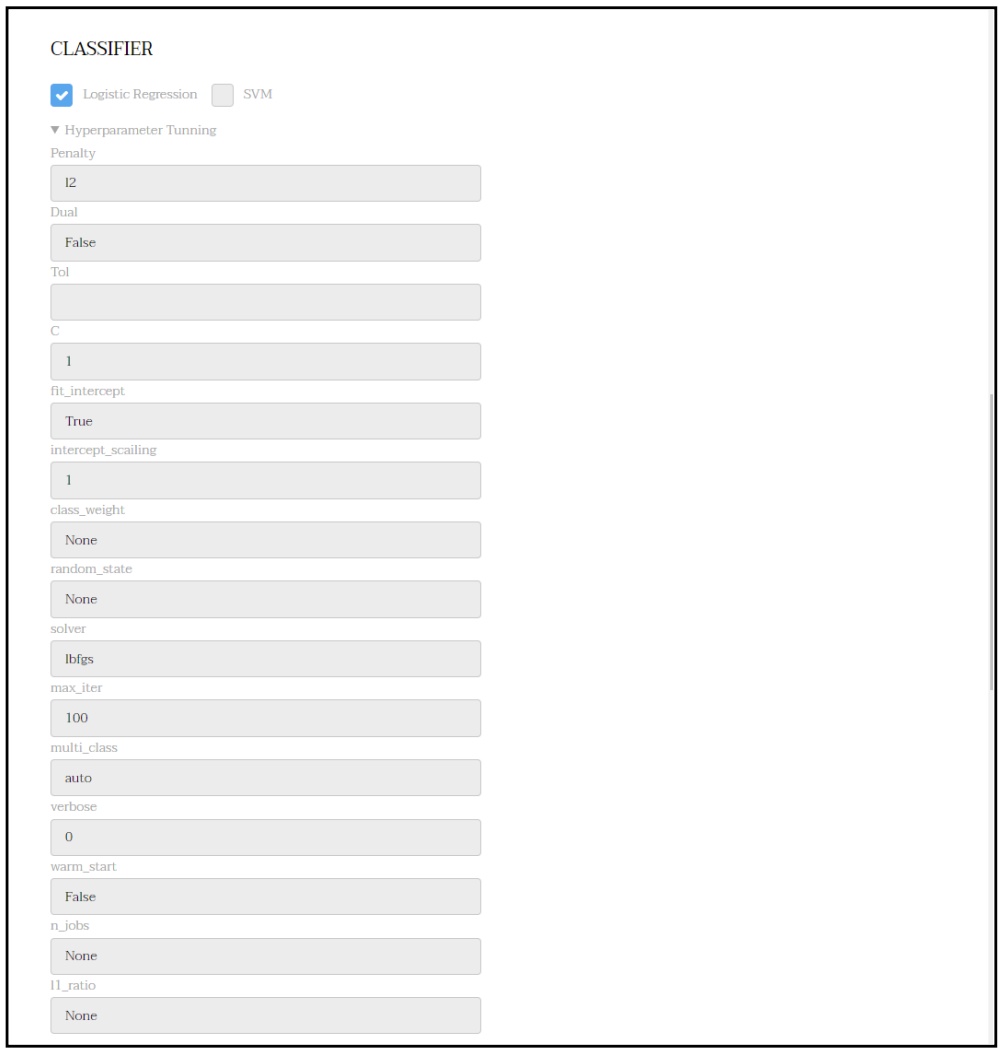

Finally, in the Prediction section, user can evaluation the selected feature to the train or test data with ROC curve and AUROC values. The web application requires which features to fit and predict, which does not have to be features selected by the application but any combination of the features that are provided in the dataset, combination of features, formatted exactly as results from feature selection must be written on the feature textbox. After choosing which estimator to proceed same as Feature selection section, user can upload train and/or test data set

to observe the performance. With the uploaded data, the application will fit the train data with provided features and present ROC curve and AUROC value in the corner, where test data prediction performance will appear under the train set result (Figure 2-5).

Figure 2-5 Prediction Page

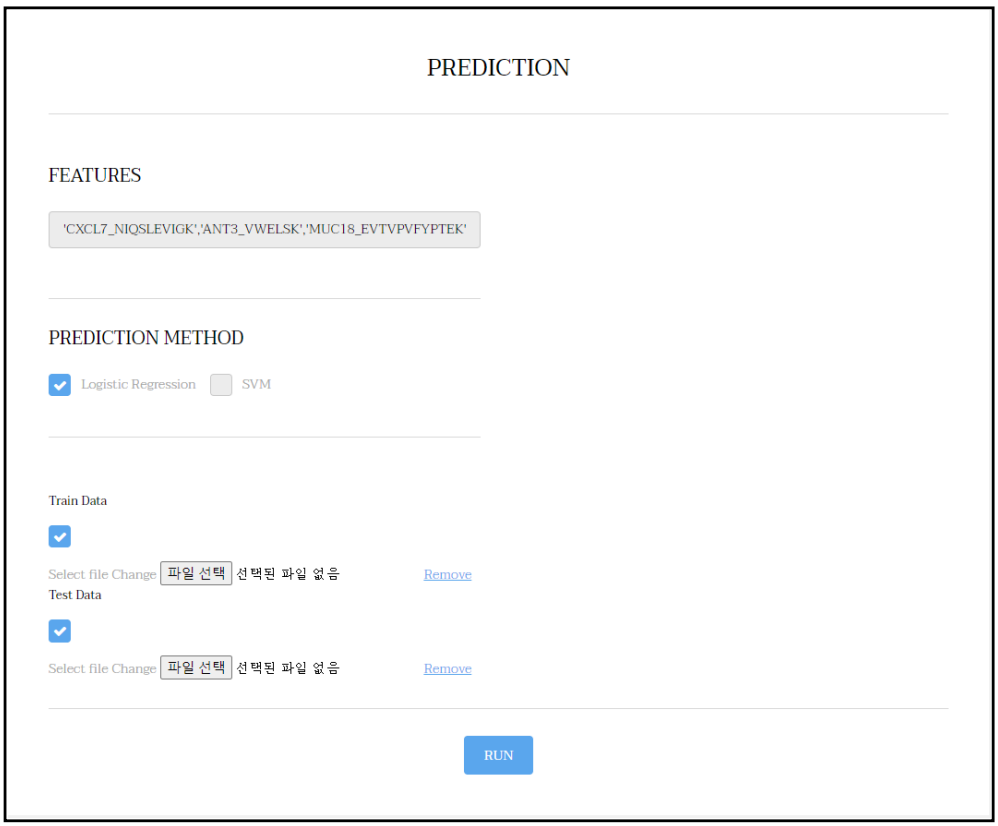

2.3.2 Method Validation Portal

The main objective of method validation is to test the reliability of the method presented by the researcher for determining one or more analyte concentration in a specific biological matrix (Figure 2-6). For the method to be considered reproducible and reliable, FDA, EMA and kFDA provides 11 criteria, some of

which across administrations, that must be fulfilled for validation. The categories are: Calibration Curve, Specificity, Sensitivity, Carryover, Precision, Accuracy, Matrix effects, Recovery, Dilution integrity, Stability, and Quality Control. Calibration Curve needs to be examined to show the linearity of quantitation range of the assay that can be expected in the study. Specificity of the method requires that target analyte and Internal standards are distinguishable from the endogenous components in the matrix with confidence. Lower Limit of Quantification (LLOQ) point of the calibration curve for each analyte defines the sensitivity of the method. Validating Carryover insures that if a high concentration of analyte in a matrix in measured, the data of the following batch will not be affected by it. Precision and Accuracy, which are self-explanatory, validates the method by assessing closeness of repeated individual measures of analytes and closeness of the observed value to the nominal value. Matrix effects are a crucial factor to account for when a method is performed by LC-MS for ion suppression or enhancement may occur during the experiment and impacts on the results. Recovery of the method requires optimization to ensure the extraction of analyte is efficient and reproducible. Dilution Integrity is a category to ensure diluting the matrix or the analyte does not impact the accuracy and precision. Stability is a category that determine the analyte in the matrix are stable during the handling and storage. Finally, QC evaluate the performance of the method and the stability of the target analyte. The detailed methods and assays are described in detail in our previous study 17. For every category, administrations have specified conditions to pass the standard, and the portal automatically calculates from the uploaded data corresponding to each category and present both calculated values and evaluation results on individual pages.

Figure 2-6 M-MVP homepage for simple and advanced analytical method validation of MRM-MS assays

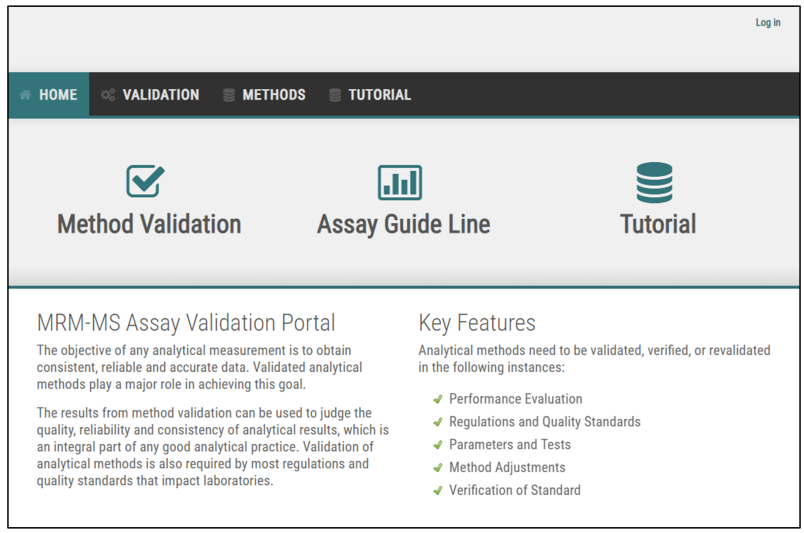

Results pages are divided into two parts: calculation and method evaluation pages (Figure 2-7).

Figure 2-7 Overview of M-MVP

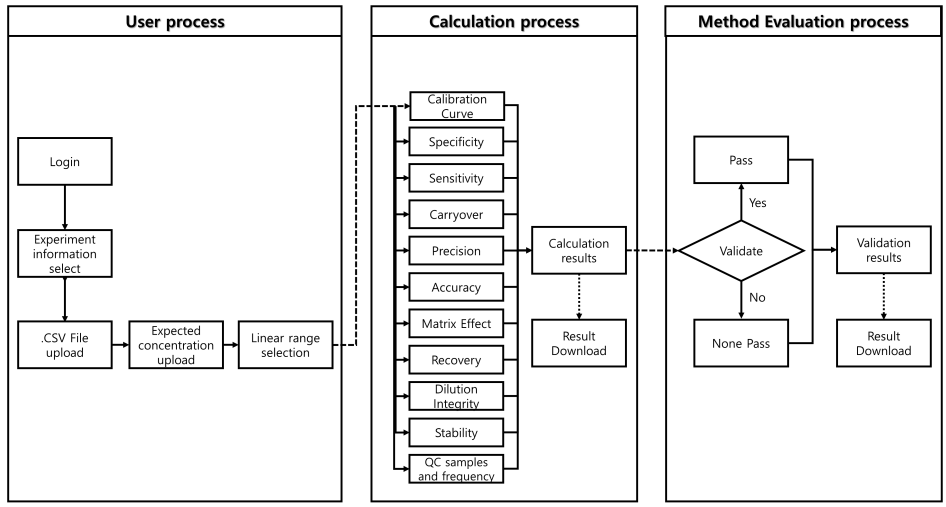

For calculation pages, the calculated results are shown in table form, in which peptide sequence, fragment, product charge, and replicate name are set as default column descriptions. Calculated values, such as averaged Peak Area Ratio (PAR) and standard deviation, are shown if required by the category (Figure 2-7). In the table, the results are shown in list form, and 10 lines and a maximum of 100 rows can be observed in a table. To save the results for personal use, M-MVP supports downloading of the table as a csv file (Figure 2-9).

Figure 2-8 Linear Regression result page

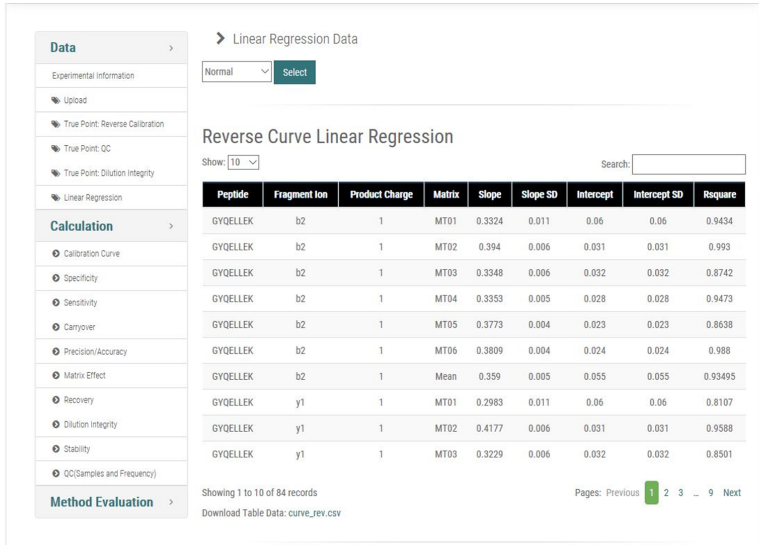

For method evaluation pages, when the user requests the calculation pages, the server will evaluate if the current categories pass the performance specification of three regulatory agencies (FDA, EMA, and KFDA) and will then store the result, along with the uploaded data. The user must examine each category to determine whether M-MVP result for a category satisfies the specified guideline. After examining all 11 categories, the user can check to see if the categories pass the performance specifications and validation practices by displaying “Pass” or “Not Pass” or “Not Addressed” if the regulatory agency did not specify a certain standard (Figure 2-10). Evaluation is performed based on the guidelines from all three regulatory agencies and the results are shown in a single table. When one or several categories fail to pass the evaluation, the user must revise the relevant category in the experiment and then upload the revised csv file.

Figure 2-9 Calibration curve result page

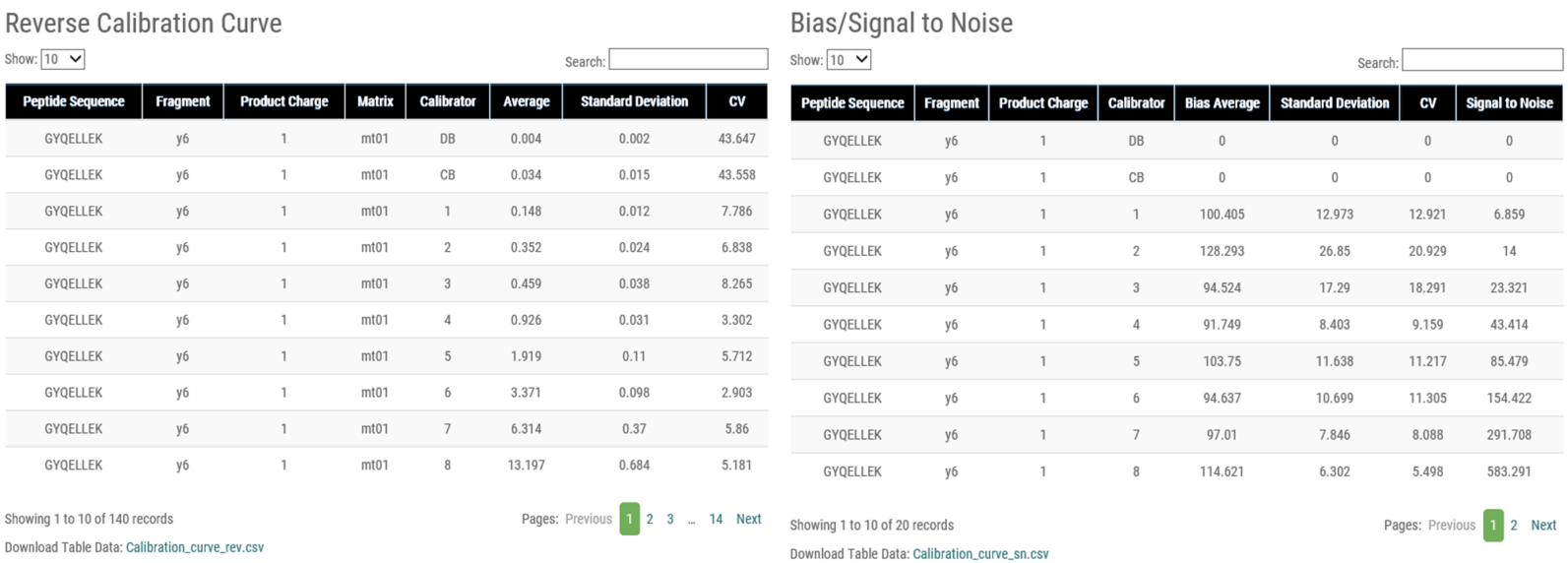

Reverse Calibration Curve

Show: 10 Search:

Peptide Sequence	Fragment	Product Charge	Matrix	Calibrator	Average	Standard Deviation	CV
GYQELLEK	y6	1	mt01	DB	0.004	0.002	43.647
GYQELLEK	y6	1	mt01	CB	0.034	0.015	43.558
GYQELLEK	y6	1	mt01	1	0.148	0.012	7.786
GYQELLEK	y6	1	mt01	2	0.352	0.024	6.838
GYQELLEK	y6	1	mt01	3	0.459	0.038	8.265
GYQELLEK	y6	1	mt01	4	0.926	0.031	3.302
GYQELLEK	y6	1	mt01	5	1.919	0.11	5.712
GYQELLEK	y6	1	mt01	6	3.371	0.098	2.903
GYQELLEK	y6	1	mt01	7	6.314	0.37	5.86
GYQELLEK	y6	1	mt01	8	13.197	0.684	5.181

Showing 1 to 10 of 140 records

Pages: Previous 1 2 3 … 14 Next

Download Table Data: Calibration_curve_rev.csv

Bias/Signal to Noise

Show: 10 Search:

Peptide Sequence	Fragment	Product Charge	Calibrator	Bias Average	Standard Deviation	CV	Signal to Noise
GYQELLEK	y6	1	DB	0	0	0	0
GYQELLEK	y6	1	CB	0	0	0	0
GYQELLEK	y6	1	1	100.405	12.973	12.921	6.859
GYQELLEK	y6	1	2	128.293	26.85	20.929	14
GYQELLEK	y6	1	3	94.524	17.29	18.291	23.321
GYQELLEK	y6	1	4	91.749	8.403	9.159	43.414
GYQELLEK	y6	1	5	103.75	11.638	11.217	85.479
GYQELLEK	y6	1	6	94.637	10.699	11.305	154.422
GYQELLEK	y6	1	7	97.01	7.846	8.088	291.708
GYQELLEK	y6	1	8	114.621	6.302	5.498	583.291

Showing 1 to 10 of 20 records

Pages: Previous 1 2 Next

Download Table Data: Calibration_curve_sn.csv

In the process of designing M-MVP on a working server, one of the main priorities was to implement an MRM-MS assay for AFP-L3, diagnosing well-known diagnostic biomarker of hepatocellular carcinoma 17. As a working example, the analytical method for M-MVP was verified using the data from the previous assay experiments, for all categories of method validation experiment was performed for the assay and already verified with standards from 3 administrations. With Skyline output data for the 11 categories, we developed and tested the performance of M-MVP of the study. The performance specifications and validation practices of the categories are embodied in M-MVP and are represented in the shape of the resulting tables, in which the format of input data and guideline details are adopted from the supplemental tables that were created for the previous study17. Furthermore, the performance specifications of the calculations that were performed by M-MVP were compared to that of a manual method using Excel with the same data. The M-MVP calculations agreed with Excel values up to 4 decimal points, at which point differences were insignificant. In terms of the time that was required for performance and validation, M-MVP completed all categories instantaneously, whereas the manual process of calculation and validation in Excel took several hours. All data for the 11 categories of the MRM-MS AFP-L3 assay are in the Tutorial tab, where users can access these data for self-education.

Figure 2-10 Method Evaluation Page

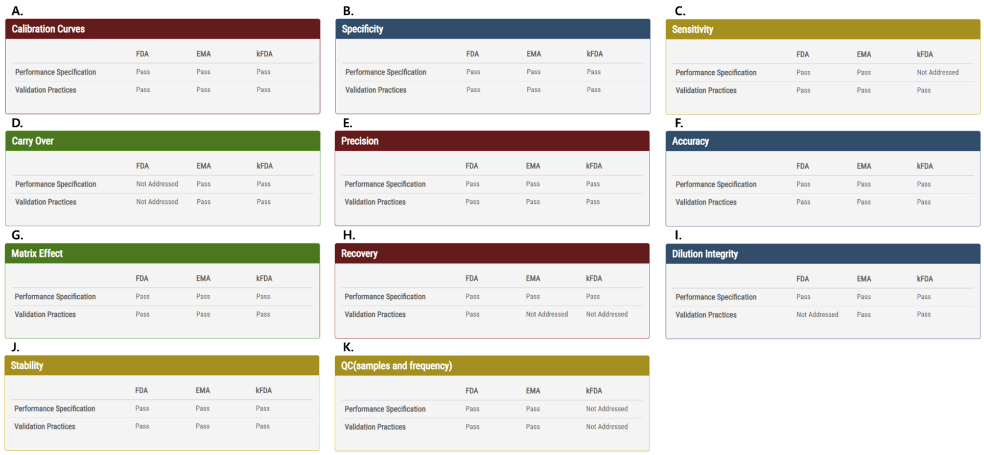

2.4. Discussion

We developed WMD for multi marker panel development and M-MVP for validating the MRM-MS assay using Skyline data. For the time-consuming nature of Machine learning methods, WMD was developed as web application but aimed to work at local terminal of the user. M-MVP, as an online assay portal, calculations are performed on the server side, which lowers the computational burden on users. Our web application aims to support the panel development and analytical validation of the MRM-MS assay. WMD have simplified the data normalization and feature selection process where M-MVP is especially effective for processing large sets of MRM-MS data, such as data that are generated with a multi-marker panel assay.

Several issues require further development. WMD, as a preliminary marker panel development tool, offers basic but essential functions to present combination of biomarkers from the uploaded data. The batch effect correction offered in this application is a method which frequently used in microarray study with limited data size(112). Many other libraries like Liger utilize various methods are offered for both R and Python(110). Unfortunately, many libraries offer for R are not supported for Python at the time being, and some Python library have not updated their library to be compatible with other libraries, resulting not able to run several libraries at same time.

A summarizing table and figure for each step might be a great assist to the researcher. Version 1.0 of WMD only shows final data results for each step, not telling what have changed or how have it calculated and transformed. It would be a

great addition to the WMD if there is an intuitive summary of how batch effect correction changed the data distribution for examples.

Feature selection is the core function of WMD. Scikit-learn offers forward, backward and RFE as wrapper methods at the time being. Stepwise features selection, which is one of most popular method, are not supported. WMD only implanted methods that are included in the Scikit-learn package, which we hope an addition of methods might be introduced and implanted in WMD.

As for MVP, the current build is sensitive to naming parameters and requires that the dataset follow the naming conventions of Skyline-generated csv files. Therefore, the user needs to ensure that uploaded files have the correct naming format that is required by M-MVP. Developing a flexible naming functionality may decrease the learning curve for users.

Implementing M-MVP into the external tools of the Skyline software site is another plausible option for development. Implementing the core functionality of M-MVP into Skyline's external tool would drastically reduce the time that is required for validation of the MRM-MS assay, because the process would run immediately on the Skyline site. Even if using M-MVP as external tool for Skyline requires more computing power from the user, he or she would not have to move files from the Skyline site to our portal and perform the entire process on a local computer. This process will ultimately lead to automation of the analytical method validation process of the MRM-MS assay.

2.5. Conclusion

Rapid advances in the sensitivity and selectivity of mass spectrometry will result in successful development of MRM-MS-based multi-marker assays. To facilitate this technology to its maximum, handling the resulting data are as much crucial as accurate and reproducible analysis method. The founding idea of WMD was to simplify the data handling process to lower the barrier for researcher to develop statistically significant assay model to reach clinical standard. With more implantation of machine learning in the diagnosis study, we look forward more clinical researchers to discover various results.

The main purpose of developing M-MVP was to facilitate the introduction of MRM-MS-based multi-marker assay into commercial sectors. Naturally, the assay development process must abide by the multinational guidelines. We hope that M-MVP will accelerate the implementation of the MRM-MS assay in clinical applications by lowering clinical entry barriers.

Furthermore, we expect that M-MVP will be applicable for metabolomics research of small molecules and chemicals, for which relevant assays will require analytical method validation.

General Conclusion

The ‘omics’ studies have been developed and conducted for many decades with the advance of computational power. Typically for proteomics, mass spectrometry has made it possible to screen thousands of proteins in a limited amount of biological material. Even more, MRM methods could have quantified targeted proteins in nanogram level, which made it possible for researchers to test its ability in the clinical area. To the present day, MRM-MS have been proved with High sensitivity and specificity, reproducible result with multiplexing capability.

Blood is one of most frequently tested clinical source since it represents the systemically complex human body with minimum invasiveness. Around the world, blood is also one of the most collected human material, which made it more accessible then other human material for researcher to develop diagnostic and prognostic methods. With above mentioned advantages, developing an assay which analyze human serum protein with MRM-LC/MS could benefit clinical diagnosis area. In chapter 1, we have developed a clinically applicable 17 protein marker panel for the early detection of HCC using chronically separated cohorts, which the performance was overwhelming compare to conventional methods and relatively advanced method called GALAD score.

While developing an MRM-LC/MS method, many computational obstacles were faced. Data manipulation and machine learning methods had to be experienced prior to data collection to develop a statistically significant model, which is one of the great challenges for many researchers with potential data to present a clinically applicable assay. In chapter 2, we have presented an user

friendly web application called WMD for those researchers who are unfamiliar with machine learning to process the data and glimpse a potential multi marker panel. Not only for beginners, WMD also provides hyperparameter tuning option for advanced users to optimize their result.

To present an analytical method to the clinical area, administrations have announced standard procedures for specific categories to prove the newly developed analytical method are reproducible and stable. For a multiplexed panel method, the administration requires validation result of each category for every single target in the panel, which not only made it frustrating for researchers to conduct each experiment, but to manipulate and calculate the resulting data according to the validation guide. The MVP web application have simplified the calculation and evaluation procedure with a single upload of the data for each category, which could have saved time and cost but more importantly it could have eliminated human error.

Overall, in this thesis, a multi marker panel were developed using mass spectrometry-based method. During the development of the panel, computational process were complicated, which lead to the idea of creating user friendly web application to aid the researchers to develop a clinically applicable panel with less frustration.

References

1. Arnold M, Abnet CC, Neale RE, Vignat J, Giovannucci EL, McGlynn KA, et al. Global burden of 5 major types of gastrointestinal cancer. Gastroenterology. 2020;159(1):335-49. e15.
2. McGlynn KA, Petrick JL, El-Serag HB. Epidemiology of hepatocellular carcinoma. Hepatology. 2021;73:4-13.
3. Liotta LA, Ferrari M, Petricoin E. Clinical proteomics: written in blood. Nature. 2003;425(6961):905.
4. Rifai N, Gillette MA, Carr SA. Protein biomarker discovery and validation: the long and uncertain path to clinical utility. Nat Biotechnol. 2006;24(8):971-83.
5. Picotti P, Bodenmiller B, Mueller LN, Domon B, Aebersold R. Full dynamic range proteome analysis of S. cerevisiae by targeted proteomics. Cell. 2009;138(4):795-806.
6. Huttenhain R, Malmstrom J, Picotti P, Aebersold R. Perspectives of targeted mass spectrometry for protein biomarker verification. Curr Opin Chem Biol. 2009;13(5-6):518-25.
7. Zhang B-H, Yang B-H, Tang Z-Y. Randomized controlled trial of screening for hepatocellular carcinoma. Journal of cancer research and clinical oncology. 2004;130(7):417-22.
8. Wu C-Y, Hsu Y-C, Ho HJ, Chen Y-J, Lee T-Y, Lin J-T. Association between ultrasonography screening and mortality in patients with hepatocellular carcinoma: a nationwide cohort study. Gut. 2016;65(4):693-701.
9. Mittal S, Kanwal F, Ying J, Chung R, Sada YH, Temple S, et al. Effectiveness of surveillance for hepatocellular carcinoma in clinical practice: a United States cohort. Journal of hepatology. 2016;65(6):1148-54.
10. Kim H, Nam J, Lee JH, Lee H, Chang Y, Lee H, et al. Intensity of surveillance for hepatocellular carcinoma determines survival in patients at risk in a hepatitis B-endemic area. Alimentary pharmacology & therapeutics. 2018;47(11):1490-501.
11. van Meer S, Robert A, Coenraad MJ, Sprengers D, van Nieuwkerk KM, Klümpen H-J, et al. Surveillance for hepatocellular carcinoma is associated with increased survival: results from a large cohort in the Netherlands. Journal of hepatology. 2015;63(5):1156-63.
12. Tzartzeva K, Obi J, Rich NE, Parikh ND, Marrero JA, Yopp A, et al. Surveillance imaging and alpha fetoprotein for early detection of hepatocellular carcinoma in patients with cirrhosis: a meta-analysis. Gastroenterology. 2018;154(6):1706-18. e1.
13. Singal AG, Lampertico P, Nahon P. Epidemiology and surveillance for hepatocellular carcinoma: New trends. Journal of Hepatology. 2020;72(2):250-61.
14. Toyoda H, Kumada T, Osaki Y, Oka H, Urano F, Kudo M, et al. Staging hepatocellular carcinoma by a novel scoring system (BALAD score) based on serum markers. Clinical Gastroenterology and Hepatology. 2006;4(12):1528-36.
15. Johnson PJ, Pirrie SJ, Cox TF, Berhane S, Teng M, Palmer D, et al. The detection of hepatocellular carcinoma using a prospectively developed and validated model based on serological biomarkers. Cancer Epidemiology and Prevention Biomarkers. 2014;23(1):144-53.
16. Best J, Bechmann LP, Sowa JP, Sydor S, Dechene A, Pflanz K, et al. GALAD Score Detects Early Hepatocellular Carcinoma in an International Cohort of Patients With Nonalcoholic Steatohepatitis. Clin Gastroenterol Hepatol. 2020;18(3):728-35 e4.
17. Liu M, Wu R, Liu X, Xu H, Chi X, Wang X, et al. Validation of the GALAD Model and Establishment of GAAP Model for Diagnosis of Hepatocellular Carcinoma in Chinese Patients. J Hepatocell Carcinoma. 2020;7:219-32.
18. Schotten C, Ostertag B, Sowa JP, Manka P, Bechmann LP, Hilgard G, et al. GALAD Score Detects Early-Stage Hepatocellular Carcinoma in a European Cohort of Chronic Hepatitis B and C Patients. Pharmaceuticals (Basel). 2021;14(8).
19. Sachan A, Kushwah S, Duseja A. GALAD Score for HCC Screening and Surveillance. Clin Gastroenterol Hepatol. 2022.

20. Singal AG, Tayob N, Mehta A, Marrero JA, El-Serag H, Jin Q, et al. GALAD demonstrates high sensitivity for HCC surveillance in a cohort of patients with cirrhosis. Hepatology. 2022;75(3):541-9.
21. Aktie R. FDA grants Breakthrough Device Designation for Roche's Elecsys GALAD score to support earlier diagnosis of hepatocellular carcinoma.
22. Shin J, Song S-Y, Ahn H-S, An BC, Choi Y-D, Yang EG, et al. Integrative analysis for the discovery of lung cancer serological markers and validation by MRM-MS. PloS one. 2017;12(8):e0183896.
23. Bhardwaj M, Gies A, Weigl K, Tikk K, Benner A, Schrotz-King P, et al. Evaluation and validation of plasma proteins using two different protein detection methods for early detection of colorectal cancer. Cancers. 2019;11(10):1426.
24. Chi L-M, Hsiao Y-C, Chien K-Y, Chen S-F, Chuang Y-N, Lin S-Y, et al. Assessment of candidate biomarkers in paired saliva and plasma samples from oral cancer patients by targeted mass spectrometry. Journal of proteomics. 2020;211:103571.
25. Goldman R, Ressom HW, Abdel-Hamid M, Goldman L, Wang A, Varghese RS, et al. Candidate markers for the detection of hepatocellular carcinoma in low-molecular weight fraction of serum. Carcinogenesis. 2007;28(10):2149-53.
26. Bruix J, Sherman M, American Association for the Study of Liver D. Management of hepatocellular carcinoma: an update. Hepatology. 2011;53(3):1020-2.
27. Yeo I, Kim GA, Kim H, Lee JH, Sohn A, Gwak GY, et al. Proteome Multimarker Panel With Multiple Reaction Monitoring-Mass Spectrometry for Early Detection of Hepatocellular Carcinoma. Hepatol Commun. 2020;4(5):753-68.
28. Emwas A-H, Saccenti E, Gao X, McKay RT, Dos Santos VAM, Roy R, et al. Recommended strategies for spectral processing and post-processing of 1D 1 H-NMR data of biofluids with a particular focus on urine. Metabolomics. 2018;14(3):1-23.
29. DeLong ER, DeLong DM, Clarke-Pearson DL. Comparing the areas under two or more correlated receiver operating characteristic curves: a nonparametric approach. Biometrics. 1988:837-45.
30. Youden WJ. Index for rating diagnostic tests. Cancer. 1950;3(1):32-5.
31. Trevisani F, D'Intino PE, Morselli-Labate AM, Mazzella G, Accogli E, Caraceni P, et al. Serum α-fetoprotein for diagnosis of hepatocellular carcinoma in patients with chronic liver disease: influence of HBsAg and anti-HCV status. Journal of hepatology. 2001;34(4):570-5.
32. Anderson NL, Anderson NG. The human plasma proteome: history, character, and diagnostic prospects. Molecular & cellular proteomics. 2002;1(11):845-67.
33. Percy AJ, Chambers AG, Yang J, Jackson AM, Domanski D, Burkhart J, et al. Method and platform standardization in MRM-based quantitative plasma proteomics. Journal of proteomics. 2013;95:66-76.
34. Rai AJ, Gelfand CA, Haywood BC, Warunek DJ, Yi J, Schuchard MD, et al. HUPO Plasma Proteome Project specimen collection and handling: towards the standardization of parameters for plasma proteome samples. Proteomics. 2005;5(13):3262-77.
35. Addona TA, Abbatiello SE, Schilling B, Skates SJ, Mani D, Bunk DM, et al. Multi-site assessment of the precision and reproducibility of multiple reaction monitoring–based measurements of proteins in plasma. Nature biotechnology. 2009;27(7):633-41.
36. Chambers AG, Percy AJ, Simon R, Borchers CH. MRM for the verification of cancer biomarker proteins: recent applications to human plasma and serum. Expert review of proteomics. 2014;11(2):137-48.
37. Domanski D, Percy AJ, Yang J, Chambers AG, Hill JS, Freue GVC, et al. MRM-based multiplexed quantitation of 67 putative cardiovascular disease biomarkers in human plasma. Proteomics. 2012;12(8):1222-43.
38. Surinova S, Hüttenhain R, Chang C-Y, Espona L, Vitek O, Aebersold R. Automated selected reaction monitoring data analysis workflow for large-scale targeted

proteomic studies. Nature protocols. 2013;8(8):1602-19.
39. Kennedy JJ, Abbatiello SE, Kim K, Yan P, Whiteaker JR, Lin C, et al. Demonstrating the feasibility of large-scale development of standardized assays to quantify human proteins. Nature methods. 2014;11(2):149-55.
40. Singal A, Volk M, Waljee A, Salgia R, Higgins P, Rogers M, et al. Meta-analysis: surveillance with ultrasound for early-stage hepatocellular carcinoma in patients with cirrhosis. Alimentary pharmacology & therapeutics. 2009;30(1):37-47.
41. Simmons O, Fetzer DT, Yokoo T, Marrero JA, Yopp A, Kono Y, et al. Predictors of adequate ultrasound quality for hepatocellular carcinoma surveillance in patients with cirrhosis. Alimentary pharmacology & therapeutics. 2017;45(1):169-77.
42. Fattovich G, Stroffolini T, Zagni I, Donato F. Hepatocellular carcinoma in cirrhosis: incidence and risk factors. Gastroenterology. 2004;127(5):S35-S50.
43. Kim SY, An J, Lim Y-S, Han S, Lee J-Y, Byun JH, et al. MRI with liver-specific contrast for surveillance of patients with cirrhosis at high risk of hepatocellular carcinoma. JAMA oncology. 2017;3(4):456-63.
44. Pocha C, Dieperink E, McMaken K, Knott A, Thuras P, Ho S. Surveillance for hepatocellular cancer with ultrasonography vs. computed tomography–a randomised study. Alimentary pharmacology & therapeutics. 2013;38(3):303-12.
45. Park HJ, Jang HY, Kim SY, Lee SJ, Won HJ, Byun JH, et al. Non-enhanced magnetic resonance imaging as a surveillance tool for hepatocellular carcinoma: comparison with ultrasound. Journal of hepatology. 2020;72(4):718-24.
46. Farvardin S, Patel J, Khambaty M, Yerokun OA, Mok H, Tiro JA, et al. Patient-reported barriers are associated with lower hepatocellular carcinoma surveillance rates in patients with cirrhosis. Hepatology. 2017;65(3):875-84.
47. Lee Y-S, Ko E, Yoon EL, Jung YK, Kim JH, Seo YS, et al. Multiplexed Proteomic Approach for Identification of Serum Biomarkers in Hepatocellular Carcinoma Patients with Normal AFP. Journal of Clinical Medicine. 2020;9(2):323.
48. Du Z, Liu X, Wei X, Luo H, Li P, Shi M, et al. Quantitative proteomics identifies a plasma multi-protein model for detection of hepatocellular carcinoma. Scientific reports. 2020;10(1):1-13.
49. Kim H, Kim K, Yu SJ, Jang ES, Yu J, Cho G, et al. Development of biomarkers for screening hepatocellular carcinoma using global data mining and multiple reaction monitoring. PLoS One. 2013;8(5):e63468.
50. Liu H, Chen H, Wu X, Sun Y, Wang Y, Zeng Y, et al. The serum proteomics tracking of hepatocellular carcinoma early recurrence following radical resection. Cancer management and research. 2019;11:2935.
51. Fye HK, Wright-Drakesmith C, Kramer HB, Camey S, da Costa AN, Jeng A, et al. Protein profiling in hepatocellular carcinoma by label-free quantitative proteomics in two west African populations. PLoS One. 2013;8(7):e68381.
52. Hoofnagle AN, Whiteaker JR, Carr SA, Kuhn E, Liu T, Massoni SA, et al. Recommendations for the generation, quantification, storage, and handling of peptides used for mass spectrometry–based assays. Clinical chemistry. 2016;62(1):48-69.
53. Hosmer Jr DW, Lemeshow S, Sturdivant RX. Applied logistic regression: John Wiley & Sons; 2013.
54. Daniele B, Bencivenga A, Megna AS, Tinessa V. α-fetoprotein and ultrasonography screening for hepatocellular carcinoma. Gastroenterology. 2004;127(5):S108-S12.
55. Inagaki Y, Tang W, Makuuchi M, Hasegawa K, Sugawara Y, Kokudo N. Clinical and molecular insights into the hepatocellular carcinoma tumour marker des-γ-carboxyprothrombin. Liver International. 2011;31(1):22-35.
56. Di Bisceglie AM, Hoofnagle JH. Elevations in serum alpha-fetoprotein levels in patients with chronic hepatitis B. Cancer. 1989;64(10):2117-20.
57. Saito S, Ojima H, Ichikawa H, Hirohashi S, Kondo T. Molecular background of alpha-fetoprotein in liver cancer cells as revealed by global RNA expression analysis.

Cancer Sci. 2008;99(12):2402-9.
58. Yoon SY, Kim JM, Oh JH, Jeon YJ, Lee DS, Kim JH, et al. Gene expression profiling of human HBV- and/or HCV-associated hepatocellular carcinoma cells using expressed sequence tags. Int J Oncol. 2006;29(2):315-27.
59. Wang Z, Yan X. CD146, a multi-functional molecule beyond adhesion. Cancer Lett. 2013;330(2):150-62.
60. Wang J, Tang X, Weng W, Qiao Y, Lin J, Liu W, et al. The membrane protein melanoma cell adhesion molecule (MCAM) is a novel tumor marker that stimulates tumorigenesis in hepatocellular carcinoma. Oncogene. 2015;34(47):5781-95.
61. Poon RT, Chung KK, Cheung ST, Lau CP, Tong SW, Leung KL, et al. Clinical significance of thrombospondin 1 expression in hepatocellular carcinoma. Clin Cancer Res. 2004;10(12 Pt 1):4150-7.
62. Tahara D, Nakanishi T, Akazawa S, Yamaguchi Y, Yamamoto H, Akashi M, et al. Lecithin-cholesterol acyltransferase and lipid transfer protein activities in liver disease. Metabolism. 1993;42(1):19-23.
63. Long J, Chen P, Lin J, Bai Y, Yang X, Bian J, et al. DNA methylation-driven genes for constructing diagnostic, prognostic, and recurrence models for hepatocellular carcinoma. Theranostics. 2019;9(24):7251-67.
64. Bulla R, Tripodo C, Rami D, Ling GS, Agostinis C, Guarnotta C, et al. C1q acts in the tumour microenvironment as a cancer-promoting factor independently of complement activation. Nat Commun. 2016;7:10346.
65. Gold B, Merriam JE, Zernant J, Hancox LS, Taiber AJ, Gehrs K, et al. Variation in factor B (BF) and complement component 2 (C2) genes is associated with age-related macular degeneration. Nat Genet. 2006;38(4):458-62.
66. Chen HH, Tsai LJ, Lee KR, Chen YM, Hung WT, Chen DY. Genetic association of complement component 2 polymorphism with systemic lupus erythematosus. Tissue Antigens. 2015;86(2):122-33.
67. Zhao Q, Peng L, Huang W, Li Q, Pei Y, Yuan P, et al. Rare inborn errors associated with chronic hepatitis B virus infection. Hepatology. 2012;56(5):1661-70.
68. Mu D, Qin F, Li B, Zhou Q. Identification of the Sixth Complement Component as Potential Key Genes in Hepatocellular Carcinoma via Bioinformatics Analysis. Biomed Res Int. 2020;2020:7042124.
69. Borchman D, Harris EN, Pierangeli SS, Lamba OP. Interactions and molecular structure of cardiolipin and beta 2-glycoprotein 1 (beta 2-GP1). Clin Exp Immunol. 1995;102(2):373-8.
70. Jing X, Piao YF, Liu Y, Gao PJ. Beta2-GPI: a novel factor in the development of hepatocellular carcinoma. J Cancer Res Clin Oncol. 2010;136(11):1671-80.
71. Majumdar S, Gonder D, Koutsis B, Poncz M. Characterization of the human beta-thromboglobulin gene. Comparison with the gene for platelet factor 4. J Biol Chem. 1991;266(9):5785-9.
72. Castor CW, Miller JW, Walz DA. Structural and biological characteristics of connective tissue activating peptide (CTAP-III), a major human platelet-derived growth factor. Proc Natl Acad Sci U S A. 1983;80(3):765-9.
73. Castor CW, Furlong AM, Carter-Su C. Connective tissue activation: stimulation of glucose transport by connective tissue activating peptide III. Biochemistry. 1985;24(7):1762-7.
74. Yamaguchi H, Lorenz M, Kempiak S, Sarmiento C, Coniglio S, Symons M, et al. Molecular mechanisms of invadopodium formation: the role of the N-WASP-Arp2/3 complex pathway and cofilin. J Cell Biol. 2005;168(3):441-52.
75. Mouneimne G, Soon L, DesMarais V, Sidani M, Song X, Yip SC, et al. Phospholipase C and cofilin are required for carcinoma cell directionality in response to EGF stimulation. J Cell Biol. 2004;166(5):697-708.
76. Yang Y, Lhotta K, Chung EK, Eder P, Neumair F, Yu CY. Complete complement components C4A and C4B deficiencies in human kidney diseases and systemic lupus

erythematosus. J Immunol. 2004;173(4):2803-14.
77. Hemelaar J, Borodovsky A, Kessler BM, Reverter D, Cook J, Kolli N, et al. Specific and covalent targeting of conjugating and deconjugating enzymes of ubiquitin-like proteins. Mol Cell Biol. 2004;24(1):84-95.
78. Grou CP, Pinto MP, Mendes AV, Domingues P, Azevedo JE. The de novo synthesis of ubiquitin: identification of deubiquitinases acting on ubiquitin precursors. Sci Rep. 2015;5:12836.
79. Frickel EM, Quesada V, Muething L, Gubbels MJ, Spooner E, Ploegh H, et al. Apicomplexan UCHL3 retains dual specificity for ubiquitin and Nedd8 throughout evolution. Cell Microbiol. 2007;9(6):1601-10.
80. Misaghi S, Galardy PJ, Meester WJ, Ovaa H, Ploegh HL, Gaudet R. Structure of the ubiquitin hydrolase UCH-L3 complexed with a suicide substrate. J Biol Chem. 2005;280(2):1512-20.
81. Teufel M, Saudek V, Ledig JP, Bernhardt A, Boularand S, Carreau A, et al. Sequence identification and characterization of human carnosinase and a closely related non-specific dipeptidase. J Biol Chem. 2003;278(8):6521-31.
82. Parkkila S, Rajaniemi H, Parkkila AK, Kivela J, Waheed A, Pastorekova S, et al. Carbonic anhydrase inhibitor suppresses invasion of renal cancer cells in vitro. Proc Natl Acad Sci U S A. 2000;97(5):2220-4.
83. Yamada T, Miyake N, Itoh K, Igari J. Further characterization of serum amyloid A4 as a minor acute phase reactant and a possible nutritional marker. Clin Chem Lab Med. 2001;39(1):7-10.
84. Keck KJ, Breheny P, Braun TA, Darbro B, Li G, Dillon JS, et al. Changes in gene expression in small bowel neuroendocrine tumors associated with progression to metastases. Surgery. 2018;163(1):232-9.
85. Feng JT, Liu YK, Song HY, Dai Z, Qin LX, Almofti MR, et al. Heat-shock protein 27: A potential biomarker for hepatocellular carcinoma identified by serum proteome analysis. Proteomics. 2005;5(17):4581-8.
86. Megger DA, Naboulsi W, Meyer HE, Sitek B. Proteome analyses of hepatocellular carcinoma. Journal of clinical and translational hepatology. 2014;2(1):23.
87. El-Serag HB. Epidemiology of viral hepatitis and hepatocellular carcinoma. Gastroenterology. 2012;142(6):1264-73. e1.
88. Cortes C, Mohri M. Confidence intervals for the area under the ROC curve. Advances in neural information processing systems. 2004;17.
89. Duffy MJ. Tumor markers in clinical practice: a review focusing on common solid cancers. Med Princ Pract. 2013;22(1):4-11.
90. Hayes DF, Allen J, Compton C, Gustavsen G, Leonard DG, McCormack R, et al. Breaking a vicious cycle. Sci Transl Med. 2013;5(196):196cm6.
91. Horvath AR, Lord SJ, StJohn A, Sandberg S, Cobbaert CM, Lorenz S, et al. From biomarkers to medical tests: the changing landscape of test evaluation. Clin Chim Acta. 2014;427:49-57.
92. Micheel CM, Nass SJ, Omenn GS. Evolution of Translational Omics: Lessons Learned and the Path Forward. In: Micheel CM, Nass SJ, Omenn GS, editors. Evolution of Translational Omics: Lessons Learned and the Path Forward. Washington (DC)2012.
93. Biesecker LG, Green RC. Diagnostic clinical genome and exome sequencing. N Engl J Med. 2014;371(12):1170.
94. Slodkowska EA, Ross JS. MammaPrint 70-gene signature: another milestone in personalized medical care for breast cancer patients. Expert Rev Mol Diagn. 2009;9(5):417-22.
95. Khleif SN, Doroshow JH, Hait WN, Collaborative A-F-NCB. AACR-FDA-NCI Cancer Biomarkers Collaborative consensus report: advancing the use of biomarkers in cancer drug development. Clin Cancer Res. 2010;16(13):3299-318.
96. Jennings L, Van Deerlin VM, Gulley ML, College of American Pathologists Molecular Pathology Resource C. Recommended principles and practices for validating

clinical molecular pathology tests. Arch Pathol Lab Med. 2009;133(5):743-55.
97. Teutsch SM, Bradley LA, Palomaki GE, Haddow JE, Piper M, Calonge N, et al. The Evaluation of Genomic Applications in Practice and Prevention (EGAPP) Initiative: methods of the EGAPP Working Group. Genet Med. 2009;11(1):3-14.
98. Shenkier T, Weir L, Levine M, Olivotto I, Whelan T, Reyno L, et al. Clinical practice guidelines for the care and treatment of breast cancer: 15. Treatment for women with stage III or locally advanced breast cancer. CMAJ. 2004;170(6):983-94.
99. Balgley BM, Wang W, De Voe DL, Lee CS. Mass spectrometry-based tissue proteomics for cancer biomarker discovery. Per Med. 2007;4(1):45-58.
100. Moosavi SM, Shekar K, Fraser J, Smith MT, Ghassabian S. High-throughput assay for quantification of the plasma concentrations of thiopental using automated solid phase extraction (SPE) directly coupled to LC-MS/MS instrumentation. J Chromatogr B Analyt Technol Biomed Life Sci. 2016;1038:80-7.
101. Sturgeon CM, Hoffman BR, Chan DW, Ch'ng SL, Hammond E, Hayes DF, et al. National Academy of Clinical Biochemistry Laboratory Medicine Practice Guidelines for use of tumor markers in clinical practice: quality requirements. Clin Chem. 2008;54(8):e1-e10.
102. MacLean B, Tomazela DM, Shulman N, Chambers M, Finney GL, Frewen B, et al. Skyline: an open source document editor for creating and analyzing targeted proteomics experiments. Bioinformatics. 2010;26(7):966-8.
103. Egertson JD, MacLean B, Johnson R, Xuan Y, MacCoss MJ. Multiplexed peptide analysis using data-independent acquisition and Skyline. Nat Protoc. 2015;10(6):887-903.
104. Tyanova S, Temu T, Sinitcyn P, Carlson A, Hein MY, Geiger T, et al. The Perseus computational platform for comprehensive analysis of (prote)omics data. Nat Methods. 2016;13(9):731-40.
105. Tyanova S, Temu T, Cox J. The MaxQuant computational platform for mass spectrometry-based shotgun proteomics. Nat Protoc. 2016;11(12):2301-19.
106. vanRossum G. Python reference manual. Department of Computer Science [CS]. 1995(R 9525).
107. McKinney W. pandas: a foundational Python library for data analysis and statistics. Python for high performance and scientific computing. 2011;14(9):1-9.
108. Bilban M, Buehler LK, Head S, Desoye G, Quaranta V. Normalizing DNA microarray data. Curr Issues Mol Biol. 2002;4(2):57-64.
109. Lander ES. Array of hope. Nat Genet. 1999;21(1 Suppl):3-4.
110. Tran HTN, Ang KS, Chevrier M, Zhang X, Lee NYS, Goh M, et al. A benchmark of batch-effect correction methods for single-cell RNA sequencing data. Genome Biol. 2020;21(1):12.
111. Behdenna A, Haziza J, Azencott C-A, Nordor A. pyComBat, a Python tool for batch effects correction in high-throughput molecular data using empirical Bayes methods. BioRxiv. 2021:2020.03. 17.995431.
112. Johnson WE, Li C, Rabinovic A. Adjusting batch effects in microarray expression data using empirical Bayes methods. Biostatistics. 2007;8(1):118-27.
113. Feng Q, Hannig J, Marron J. A note on automatic data transformation. Stat. 2016;5(1):82-7.
114. Harris CR, Millman KJ, Van Der Walt SJ, Gommers R, Virtanen P, Cournapeau D, et al. Array programming with NumPy. Nature. 2020;585(7825):357-62.
115. Virtanen P, Gommers R, Oliphant TE, Haberland M, Reddy T, Cournapeau D, et al. SciPy 1.0: fundamental algorithms for scientific computing in Python. Nature methods. 2020;17(3):261-72.
116. Pedregosa F, Varoquaux G, Gramfort A, Michel V, Thirion B, Grisel O, et al. Scikit-learn: Machine learning in Python. the Journal of machine Learning research. 2011;12:2825-30.
117. Johnson R, Hoeller J, Donald K, Sampaleanu C, Harrop R, Risberg T, et al. The spring framework–reference documentation. interface. 2004;21:27.

118. Arnold K, Gosling J, Holmes D. The Java programming language: Addison Wesley Professional; 2005.
119. Flanagan D, Novak GM. Java-Script: The Definitive Guide. American Institute of Physics; 1998.
120. Garrett JJ. Ajax: A new approach to web applications. 2005.
121. Widenius M, Axmark D, Arno K. MySQL reference manual: documentation from the source: " O'Reilly Media, Inc."; 2002.
122. Muschko B. Gradle in action: Simon and Schuster; 2014.
123. Kim H, Sohn A, Yeo I, Yu SJ, Yoon JH, Kim Y. Clinical Assay for AFP-L3 by Using Multiple Reaction Monitoring-Mass Spectrometry for Diagnosing Hepatocellular Carcinoma. Clin Chem. 2018;64(8):1230-8.

국 문 초 록

서론: 전통적인 간세포암의 감시진단은 이미징 기법과 혈청 종양 마커의 정량으로 진단하나, 충분치 못한 정확성의 한계가 있다. 간세포암 조기진단에 대한 수요는 존재하며, 본 실험에서는 이를 프로테오믹 기술 기반 혈청 분석 바이오마커 패널의 제작 및 검증을 통해 정확성이 향상된 기법을 제시한다. 또 한 이러한 바이오마커 패널의 임상적용을 위한 바이오마커 개발과 분석법 검증의 전산작업을 직관적으로 진행 할 수 있는 두개의 웹 어플리케이션을 개발 및 제시한다.

방법: 1장에서는 다기관 환자 대조군 시료는 간세포암 환자군과 간경화증, 만성 B형 간염, 만성 C형 간염등을 보유 하나 간세포암이 아닌 집단군이다. 본 실험은 질량분석기 다중반응검지법기반의 17 단백질 바이오마커를 398명의 환자 대조군으로 개발하였다. 알파태아닌 단백질, 비타민 K 길항제-II를 개발된 패널의 마커에 더 했을때의 성능을 곡선 아래 면적으로 확인하였으며, 이를 398명의 학습데이터와 170명의 평가데이터, 시간적으로 단절된 159명의 검증 데이터로 검증하였다. 2장에서 바이오마커 개발 웹 어플리케이션은 파이썬 언어와 Scikit-Learn 모듈로 개발하였으며, Django Framework로 웹 어플리케이션의 틀을 구성하였다. 배치 효과 정규화와 데이터 치우침 기반 정규화 기능을 제공하며, 전진선택법, 후진선택법 및 Recursive Feature Elimination 기법을 바이오마커 선정 기능으로 개발하였다. 머신러닝 평가 기능은 로지스틱 회귀 기법과 서포트 벡터 머신 기법을 채용하였다. 분석법 평가 포탈은 Spring boot로 웹 어플리케이션 기반을 확립했으며, JSP, HTML, JavaScript를 프론트단을 개발하였다. 아파치 톰캣, MySQL로 서버의 개발과 데이터베이스를 개발하였다

결과: 1장에서는 알파태아닌 단백질, 비타민 K 길항제-II를 추가한 패널에서 곡선 아래 면적의 수치가 패널 단일일 때보다 높은 것을 학습데이터 (0.989 vs 0.937, $P<0.05$)와 검증데이터 (0.958 vs 0.940, $P<0.05$)에서 확인하였으나 평가데이터 (0.898 vs 0.891, $P=0.28$)에서 하락함을 확인하였다. 조합 및 단일 패널에서 모두 현행 알파태아닌단백질 단독 마커에 비해 2센치 이하의 단일 간세포암

환자군 구별에 있어 높은 곡선 아래 면적 수치을 학습데이터 (0.940 & 0.929 vs 0.775, 모두 P<0.05), 평가 데이터 (0.894 & 0.893 vs 0.593, 모두 P<0.05), 검증데이터 (0.961 & 0.937 vs 0.806, 모두 P<0.05)에서 확인 할 수 있었다. 조합 및 단일 패널에서 모두 GALAD score 보다 높은 곡선 아래 면적 수치를 확인 할수 있었다(0.945 and 0.931 vs 0.829, 모두 P<0.05). 제 2장에서는 WMD는 데이터 전처리, 바이오마커 선정 및 개발된 모델에 대한 평가를 섹션별로 기능제공을 하는 웹 어플리케이션을 개발하였다. WMD로 개별 샘플의 타겟 정량데이터가 들어있는 2차원 데이터를 최종적으로 모델까지 개발 할 수 있음을 확인하였다. MVP 포탈은 Skyline 프로그램에서 추출된 아래 각 분석법 검증 항목의 실험 결과 데이터를 계산하고 검증 할 수 있다: 검량선, 특이성, 선택성, 캐리오버, 정확성, 생체시료 효과, 회수율, 희석의 타당성, 안정성 및 품질관리시료 항목등이 있다. 계산이 끝난 항목들의 계산 결과 및 기준 통과 여부는 관 페이지에서 확인 할 수 있다.

결론: 본 실험에서 개발한 17 단백 다중 마커 패널은 간세포암 환자를 고위험군 대조군에서 구분 할 수 있었으며 조기 발견에 높은 정확성을 보였다. 또 한 바이오마커 개발에 요구되는 전산 작업을 할 수 있는 웹 어플리케이션으로 모델 개발 과정과 분석 검증 과정을 간소화 할 수 있었다.

주요어 : 간세포암, 바이오마커, 프로테옴, 혈청, 소프트웨어

학 번 : 2018-36314